TURUN YLIOPISTO

Luminescence-based methods for cellular guanosine triphosphate (GTP)

Master's Thesis

Titta Yli-Hollo
Chemistry of Drug Development, Bioanalytical Chemistry
Department of Chemistry, Detection Technology
University of Turku

16.06.2023
Turku

Master's Thesis

Subject: Chemistry of Drug Development
Author: Titta Yli-Hollo
Title: Luminescence-based methods for cellular guanosine triphosphate (GTP)
Supervisors: PhD Kari Kopra, prof. Atsuo T. Sasaki
Number of pages: 70
Date: 16.06.2023

Guanosine triphosphate (GTP) is an important energy and signaling molecule. The cellular concentration of GTP increases in rapidly dividing cells, such as cancer cells, since GTP is needed in the translation of proteins. In cancer cells, GTP concentration in relation to adenosine triphosphate (ATP) increases significantly. Inosine-monophosphate dehydrogenases (IMPDH) are responsible for the synthesis of GTP and have attracted attention as a potential drug target, among other potential GTP sensor proteins. Thus, new techniques to study GTP and its cellular regulation would benefit the investigation of new drug targets and the development of cancer drugs. To investigate GTP, efficient binders would be beneficial, and previously, our group has successfully developed the first fragment antigen-binding (Fab) against GTP using the phage display technology. The introduced Fab2A4 has over 100-fold specificity to GTP over other purine nucleotide ATP and guanosine diphosphate (GDP). Using this antibody, a competitive assay utilizing GTP-conjugated 9-dentate Eu^{3+}-chelate has been developed for the analysis of GTP hydrolysis. In bioimaging, cellular GTP has been imaged indirectly utilizing various GTP sensors in the past. Small molecules, such as nucleotides, are difficult targets for imaging from fixed cells and require specific binders with high affinity. Additionally, the high intracellular ATP concentration sets high demands for GTP binder specificity.

In this study, the aim was to develop new methods to monitor GTP concentrations utilizing GTP-specific antibody. Two cell-based applications were developed by using the anti-GTP Fab. Firstly, the method was developed for direct GTP imaging from fixed cells with fluorescence microscopy. In bioimaging, the new maturated GTP antibody variant Fab2A4m showed improved functionality in comparison to Fab2A4. Secondly, Fab2A4 was utilized in a time-resolved luminescence-based (TRL) homogenous assay with 9-dentate Eu^{3+}-chelate for GTP and combined with ATP detection from cell lysate. The long-lived emission of lanthanide chelates enables the TRL measurements, and therefore the background autofluorescence can be eliminated, leading to high assay sensitivity. In two cell strains, both methods were used to compare cellular GTP levels after different treatments, and for imaging also the expression of GTP synthetic IMPDH2 enzyme.

Keywords: guanosine triphosphate, immunofluorescence, luminescence, lanthanide chelates

Table of contents

Abbreviations

Ab antibody

ADP adenosine triphosphate

AMP adenosine monophosphate

ATP adenosine triphosphate

BSA bovine serum albumin

CE capillary electrophoresis

cpYFP circularly permuted yellow fluorescent protein

CRISPR clustered regularly-interspaced short palindromic repeats

CTP cytosine triphosphate

CV% coefficient of variation

dGTP deoxyriboguanosine triphosphate

DKO double-knockout

DMEM Dulbecco's Modified Eagle Medium

DMF dimethylformamide

DMSO dimethyl sulfoxide

DNA deoxyribonucleic acid

EDTA ethylenediaminetetraacetic acid

FA Fluorescence Anisotropy

Fab Fragment antigen-binding

FBS Fetal Bovine Serum

FP Fluorescence Polarization

FPIA Fluorescence Polarization ImmunoAssay

GDP guanosine diphosphate

GEVAL GTP evaluator

GMP guanosine monophosphate

GPCR G-protein coupled receptor

GTP guanosine triphosphate

HEPES hydroxyethyl-piperazine-ethane sulfonic acid

HPLC High-Performance Liquid Chromatography

HTS high-throughput screening

IgG/IgM immunoglobulin G and M

IMPDH1, IMPDH2 Inosine-monophosphate dehydrogenases 1 and 2

ISC intersystem crossing

IT ion trap

ITP inosine triphosphate

KO knock-out

MALDI matrix-assisted laser desorption ionization

MPA mycophenolic acid

MQ MilliQ water

MS mass spectrometry

NTP nucleotide triphosphate

PBP phosphate-binding protein

PBS phosphate-buffered saline

PET polyethylene terephthalate

PFA paraformaldehyde

PI(5)P phosphatidylinositol 5-phosphate (PI(5)P) lipid

PI5P4Kβ, PI5P4Kγ phosphatidylinositol 5-phosphate 4-kinase β and γ

PLL poly-L-lysine

QRET Quenching Resonance Energy Transfer

RNA ribonucleic acid

RPLC Reversed-phase Liquid Chromatography

RT room temperature

ScFvM single-chain variable fragments multipurpose

TBS Tris-buffered saline

TR-FRET Time-Resolved Förster Resonance Energy Transfer

UV ultraviolet

RR Rods and Rings

TRL Time-resolved Luminescence

WT wild type

XMP xanthine monophosphate

1 Introduction

1.1 Cellular guanosine triphosphate (GTP)

Guanosine triphosphate (GTP) is a nucleotide, and it is an important energy and signaling molecule. The nucleobase of GTP is guanine, which is a purine ring. Another nucleotide triphosphate (NTP), which has purine as its nucleobase, is adenosine triphosphate (ATP). ATP is a better-known nucleotide since it is the primary energy source of cells. Nucleotides consist of three sections, nucleobase, sugar, and phosphate chain of 1 to 3 phosphate groups. GTP (M(GTP)=523,18 g/mol) and ATP (M(ATP)=507,18 g/mol) have three phosphate groups and a ribose sugar ring in the middle, and they only vary by their nucleobase. In ATP the nucleobase is adenine and in GTP the nucleobase is guanine (Figure 1).[1] Guanine and adenine are nitrogen-rich and aromatic purine bases which differs from each other by two functional groups. They consist of two heterocyclic rings. There is an amino group at position C6 in adenine and at position C2 in guanine (Figure 1). The significant difference between the bases is the ketone oxygen at position C6 in guanine. Because of this double-bonded oxygen, there is not π bond between the positions 1 and 6. The π electrons are transferred to bind the oxygen and the nitrogen at position 1 has bind an additional hydrogen. When the sugar ring (ribose or deoxyribose) binds to the nitrogen, the structure is called nucleoside. Nucleosides are precursors of nucleotides. The bond between the C1 of the ribose and N9 of the purine base is an N-glycosidic bond. When nucleoside binds to the phosphate group with an ester bond at position C5 of the sugar ring, the structure is called nucleotide.[1] Nucleotides are precursors of nucleic acids, deoxyribonucleic acid (DNA) and ribonucleic acid (RNA). The sugar ring in RNA is ribose and deoxyribose in DNA. In a double helix of DNA and RNA, purine rings bind to pyrimidine bases (cytosine and thymine or uracil) with two (adenine + thymine/uracil) or three hydrogen bonds (guanine and cytosine).[2,3]

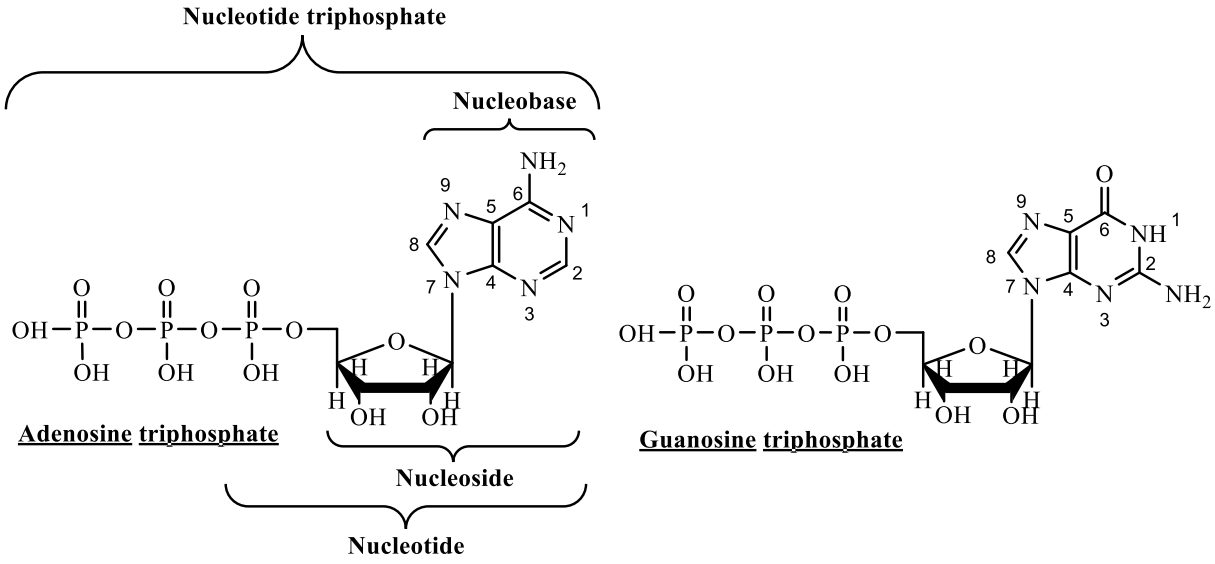

Figure 1. The chemical structure of adenosine triphosphate (ATP) and guanosine triphosphate (GTP).

Cellular nucleotides are produced first as monophosphates, like adenosine monophosphate (AMP) and guanosine monophosphate (GMP) but nucleotides are usually used as triphosphates in the cells.[1] The reversible reactions of the phosphate chain are required for the reactions which make the operations of the cells possible. The hydrolysis of the phosphate chain and the transfer of the phosphate group from nucleotide to another molecule releases the chemical energy from the ester bond.[1] The released energy can be converted for example to movement and cells can use the energy for energetically uneconomical processes, for example in active transfer through the plasma membrane (for example in the natrium-potassium pump) or the contraction of the muscles. Triphosphates have the highest energetic state, but diphosphates can also release the energy from their ester bond between two phosphate groups.

The most important energy molecules for the reversible energy processes are ATP and GTP. ATP is the main energy source in the cellular energy metabolism.[2,3] The major role of GTP is as a secondary messenger in the signaling cascades of the G-protein coupled receptors (GPCR). The conformation of the G-protein coupled receptor changes by the binding of a ligand. The conformational change activates the G-protein inside the cell and its α-moiety replaces guanosine diphosphate (GDP) with GTP. This change releases α-moiety and causes a cascade of activation reactions.[2] The abnormal functionality of the GPCRs has been identified in many diseases. The most widely studied role of GTP is in GPCRs' linkage to cancer. Approximately 30–40% of drugs are targeted against GPCRs.[4] The role of GTP is important in the synthesis of new proteins as well. In the protein translation, two GTP molecules are consumed when an amino acid is added to the polypeptide chain with an amide bond (peptide bond). Therefore, the concentration of GTP is high in the cells which are producing the serum

proteins in the liver, and in the pancreas and adipose tissue. The concentration is also increased in rapidly dividing cells, such as cancer cells, because of the active translation of new proteins.[5]

The regulation of the concentrations of the cellular energy molecules is essential for the survival of the cells. The main sensor for intracellular GTP concentration is phosphatidylinositol 5-phosphate 4-kinase β (PI5P4Kβ).[5] Its GTP sensing mechanism affects cell metabolism through the regulation of homeostasis. Another isoform, PI5P4Kγ could also have a GTP sensing role in the cells, but its enzymatic activity was 200-fold slower. The PI5P4Kβ binds to GTP directly but shares its catalytic binding site with ATP. The binding of GTP to its binding pocket with four hydrogen bonds changes the activity of the kinase, and therefore the increasing GTP concentration increases the kinase activity. The secondary messenger in the pathway is phosphatidylinositol 5-phosphate (PI(5)P) lipid. The concentration of PI(5)P is changed by the kinase based on the changes in cellular GTP. In the future, the kinase is a promising target for new cancer drugs, because the activity of the kinase increased the tumorigenesis *in vivo*. Kinase's sensing activity is critical for changes in metabolism and tumorigenesis and therefore it could represent a new target for cancer drug development.[5]

GTP is produced by two purine biosynthesis pathways, salvage and *de novo* GTP synthesis. The salvage pathway consumes nucleobase or purine nucleoside to produce purine nucleotide monophosphate. Purine synthesis via the *de novo* pathway is a highly energy-consuming process. When the salvage pathway from guanine to GTP through 3 reactions requires the energy of only 2 ATP molecules, the *de novo* pathways to GTP through 20 reactions require the energy of 9 ATP molecules. The key enzyme of the GTP *de novo* pathway is inosine monophosphate dehydrogenase (IMPDH).[6] In mammalian cells, IMPDH has two isoforms, IMPDH1 and IMPHD2, which are 84% identical in their primary sequence.[6,7] In the study of human brain cancer glioblastoma, the U87MG wild type (WT) cell line is very commonly used.[8] To study the regulation of nucleotides and the affection to tumorigenesis in the cells, U87MG IMPDH1 and IMPDH2 knockout (KO) cells and IMPDH1/2 double-knockout (DKO) cells have been produced.[9] The synthetic pathways to produce GTP has been blocked by knocking out IMPDH1/2-enzymes, which are producing the precursor xanthine monophosphate (XMP). KOs and DKO were designed and produced by utilizing the clustered regularly-interspaced short palindromic repeats (CRISPR)-Cas9 technique.[9] Interestingly, U87MG IMPDH1 KO cells did have almost similar levels of GTP to U87MG WT cells due to

compensation. The U87MG IMPDH2 KO reduced the GTP level more effectively and IMPDH1/2 DKO cells even more (measured by high-performance liquid chromatography, HPLC). Based on this, IMPDH2 reprograms the GTP metabolism and is critical for *de novo* GTP synthesis in glioblastoma cells.[9,6] In addition to the genetic inhibition, the GTP level can also be inhibited pharmacologically with mycophenolic acid (MPA).[9,6,7,10,11] MPA is an IMPDH inhibitor, which traps a covalent intermediate of IMPDH with covalently bound nucleotide and therefore inhibits the step in the synthetic pathway of guanosine triphosphate.[11] MPA treatment decreases the GTP level and possibly can increase the ATP level or have no effect on ATP. IMPDH activity is characteristic in glioblastoma cells and requirement for tumorigenesis since IMPDH DKO cells failed to form tumours. On the other hand, the GTP concentration in primary glia cells were not affected by MPA treatment.[9]

In bioimaging, MPA induces rods and rings (RRs) effect on IMPDH enzymes.[10,7] RRs are fibrous but reversible structures in cytoplasm and their shape is a complex of linear and rounded rods. RRs form as a result of the homopolymerization of IMPDH.[7] Strong formation of IMPDH2 RRs for example in HeLa cells by 1 μM MPA for 2–4 h has been reported with immunofluorescence and also with silver-enhanced electron microscopy.[7,11] The time to reach the maximum RR formation varied between different cell lines and the RR effect had also exceptional cell lines. Also under glucose starvation, the formation of RRs has been reported to be slower. Simultaneous addition of guanosine has been reported to prevent the formation of RRs and shown the RR formation to be a reversible process. Possibly, guanosine compensates for the nucleotide production via the purine salvage pathway, when MPA is inhibiting the *de novo* pathway.[7] The results with fibroblast cells, which can not convert guanosine to nucleotides (Lesch-Nyhan disease), suggest that the reversible RR unfolding is not caused straight by the guanosine, but rather by guanine nucleotides.[7,11]

There is a little amount of free nucleotides in the cells and free nucleotides are produced for a certain need,[2] like contraction of the muscle fiber or protein translation. Also, the production of nucleotides is strictly regulated in the cells. The concentration of ATP varies approximately between 1000–5000 μM and the concentration of GTP approximately 100–1000 μM and concentrations of the respective diphosphates are approximately adenosine diphosphate (ADP) 140 μM and GDP 40 μM in human cells.[12] The concentrations vary widely depending on the cell type, origin (tumor, normal tissue or cultured cells) and the environment of the cells.[5,12] However, there has not been an established way of reporting the amounts of nucleotides in the samples. The comparison of the reported nucleotide concentrations is

therefore problematic. The concentration can be reported as the amount of substance or concentration per 10^6 or 10^9 cells, and sometimes per sample volume in mL. One source of error is also the volume of cells used in calculations. The average volume used for the results of the review was 2.56 ± 1.3 mL/10^9 cells (excluding erythrocytes). Another factor causing error in the results is the labile nature of the triphosphates. The contamination of the samples containing triphosphates appears easily, because of the degradation caused by the enzymes in the environment.[12] To prevent this, the addition of Tris-Cl[13] or EDTA[14] in the buffer solution could reduce the hydrolysis of triphosphates during the sample preparation.

When compared to the normal tissue, the ATP concentration is 1.2 times higher and the GTP concentration is 2.0 times higher in tumor cells and the concentration of cytosine triphosphate (CTP) increases 4.8 times in tumor cells.[12] Nevertheless, CTP is a poor indicator for diseases, since the concentration of CTP in normal tissue is low, below 100 µM (92 ± 34 µM)[12] and therefore harder to measure accurately. The concentration of ATP increases in tumor cells, but it is high in normal cells as well.[12] Therefore the change in GTP concentration is the most suitable indicator among the nucleotides for the possible disease and describes well the energy metabolic state of the cells. The ratio of ATP and GTP gives more widely information of the energetic state of the cells. Based on the review article, the ATP-GTP ratio is approximately 10.9 in the cells of the cell culture, 7.5 in tissue and 6.6 in tumor cells.[12] The ratio decreases in tumor cells because of the increased GTP concentration.

The cellular GTP concentration can be measured in different ways. Traditional separation-based techniques are commonly used and shortly described further. Luminescence-based techniques are discussed more widely because of their advantages and strong potential and because of the connection to the luminescent techniques used in the experimental section.

1.2 Luminescent techniques for GTP

In this section luminescent techniques are discussed, and lanthanide chelates are introduced. First fluorescence and intersystem crossing are described, and then the properties of lanthanides and delayed luminescence are introduced. Next, assay properties of dyes are discussed, and one specific lanthanide chelate is introduced. Lastly two fluorescent techniques are discussed more detail.

Luminescence is the emission from a compound which has been exposed to light or electromagnetic radiation. Fluorescence is a type of luminescence, in which the relaxation

occurs in a short period of time. Fluorescence requires that the molecule can be excited by the quantum energy of the photon to the singlet states S_1 and S_2 (Figure 2). In the short lifetime fluorescence emission, the energy of the electron of the molecule is emitted when the electron returns back to the ground state.[15] Intersystem crossing (ISC) is a process where the spin of the excited electron is reversed and in the triplet state T the spin of the excited electron is the same (parallel) with its electron pair (Figure 2). ISC process can occur if the vibrational levels of the two excited states overlap. Energy is not lost in this transition.[4]

Lanthanides belong to the group of rare-earth metals. For example, samarium $_{62}Sm^{3+}$, europium $_{63}Eu^{3+}$, terbium $_{65}Tb^{3+}$ and dysprosium $_{66}Dy^{3+}$ are lanthanide ions which can act as a center ion in the chelate structure.[4] In a structure of a lanthanide chelate, the lanthanide ion makes a complex with an organic chelator molecule. The energy transfer from the triplet state can occur in lanthanide chelates. From lanthanide, such as Eu^{3+}, the excitation energy can be emitted with the delayed luminescence and then it returns to the ground state.[16] Quenching is a process where luminescence decreases. With the presence of a soluble modulator molecule, the energy of the excited states of the donor molecule can be transferred to the modulator molecule and that way to the ground state. In that case, high luminescence signals of emission can not be detected anymore.

Quenching Resonance Energy Transfer (QRET) is a time-resolved luminometric method. Luminometric methods can be time-resolved or steady-state methods. Autoluminescence of the background can be eliminated with lanthanide chelates using time-resolved measurements. Lanthanide ions, such as Eu^{3+}, chelates can be used in time-resolved measurements because their emission time is long and emission differs from excitation.[16] In time-resolved measurements, the molecules are excited with photons which are carrying the energy of a certain wavelength. Equation 1 describes the energy quantum carried by one photon of a certain wavelength. The energy of the photon increases when the wavelength decreases, in the range of visible light this means from red (630–700 nm) to blue/purple (400–490 nm) light. Emission can be measured in a separate emission wavelength. Because the emission wavelength is longer than excitation, the emitted photon does not absorb again. Therefore, the emission is proportional to the concentration in a wide dynamic range.

$$E = \frac{hv}{\lambda} \quad (1)$$

A soluble modulator can quench the signal of the unbound labelled ligands and the signal of bounded labelled ligands can be measured. The labelled ligand can be for example a nucleotide or small peptide.[4] When the donor and quencher are close to each other, the emission signal can not be measured. When a ligand with lanthanide chelate bonds with its target molecule, the distance between the quencher and lanthanide chelate increases and interactions does not occur. The weak interactions between modulator molecule and Eu^{3+}-chelates bounded ligands break when the ligand is binding and the signal can not be quenched. Energy does not flow to the quencher and emission can be measured. The advantages of QRET are for example that the separation of an analyte from the sample matrix is not needed, the optical monitoring is quick, low final volumes for detection and the homogenous assay form. The homogenous methods are simpler than heterogenous, in which multiple washing steps are often needed. Therefore homogenous methods are faster and also easier to automatize for high-throughput screening (HTS) purposes.[4] The lanthanide chelate labels overcome the limitations of conventional fluorescent labels. The long-lived emission of lanthanide chelates enables the TRL measurements, and therefore the background autoluminescence can be eliminated, leading to high assay sensitivity.[16] QRET uses a single-label technique, and only the labelling of the binding molecule is needed.[4] This also increases the simplicity of the technique and its applicability for HTS purposes.

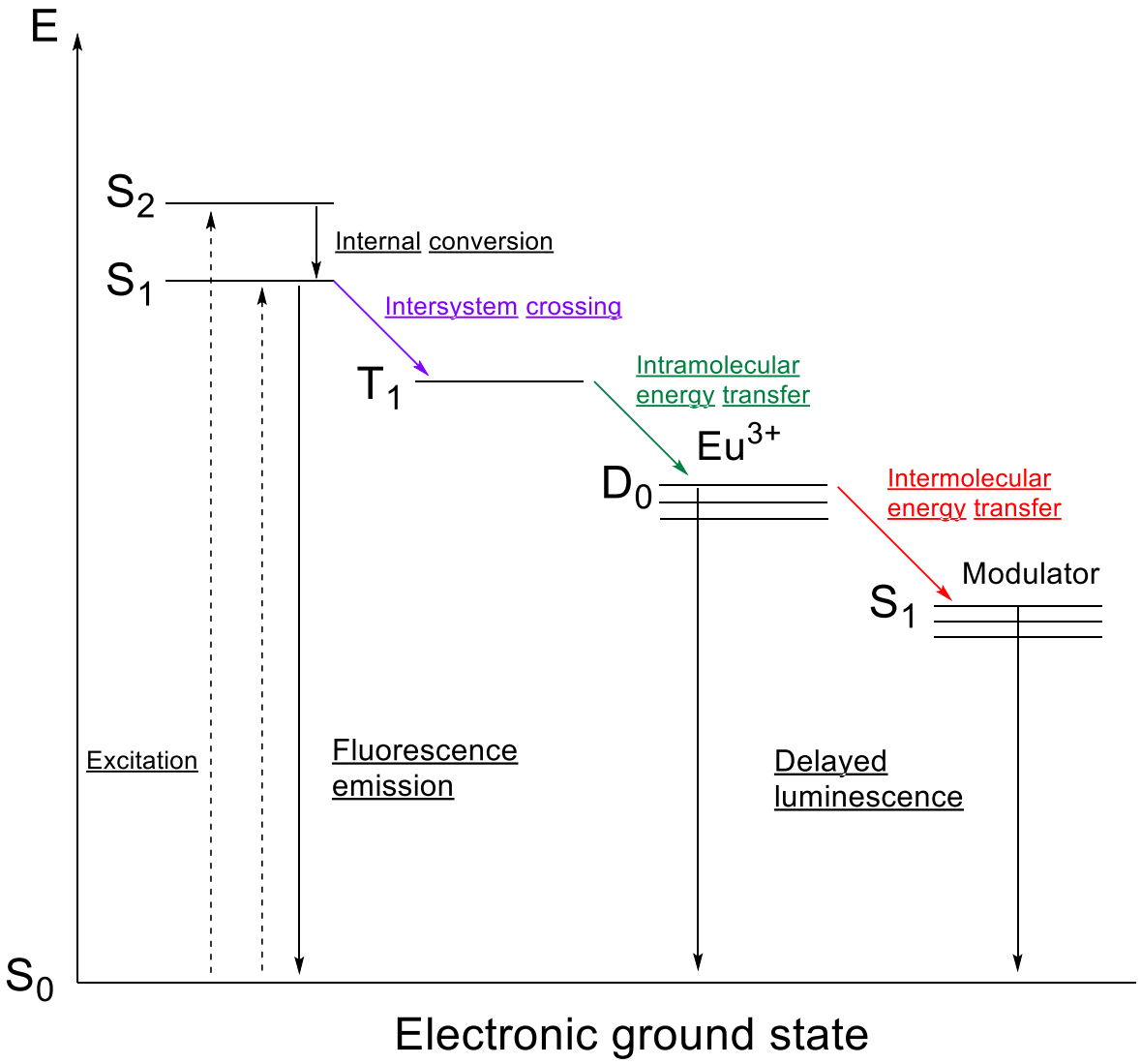

Figure 2. Energy transfer Jablonski diagram. Jablonski diagram of the transition/relaxation states.

The studied molecular interaction determines the properties of the buffer used. The conditions of the assay and the microenvironment of the probe affect the fluorescence properties of the fluorophores. For example, the pH of the solution affects quantum yield (φ), fluorescence lifetime (τ) and extinction coefficient (ε) of some fluorophores. The quantum yield of the fluorophore φ is the ratio of the amount of the emitted photons to the amount of the absorbed photons. High quantum yield is a highly desirable property of the probe, especially when studying strong affinity interactions and using low concentrations of the fluorescent probe. The assay performance can be improved by the minor addition (0.01%) of the detergent, which can reduce the surface tension and the adsorption of the proteins to the surfaces of the wells. For example, Saponin, Nonidet P40, Triton X-100 and Brij-35 are general detergents. Also, the salt concentration of the buffer needs to be optimized for each assay.[15]

The long fluorescence decay after excitation of lanthanide chelates enables time-gated detection system. The time-resolved emission with narrow emission lines eliminates the background.[16,17] Eu^{3+}-chelate 4-[2-(4-isothiocyanatophenyl)-ethynyl]-2,6,-bis{[N,N-bis(carboxymethyl)-amino]methyl}-pyridine europium(III) bearing one additional iminodiacetate coordinating arm has been developed for bioaffinity assays. The Eu^{3+}-chelate is a widely used labelling reagent since it covers well the demands for chelates used in bioaffinity assays. These requirements are for example high hydrophilicity, biocompatibility and little effect on biomolecules, small size, and stability in the presence of other chelators even at extreme conditions, such as high temperature and low pH. Also, energy transfer properties and optimal emission profile would be required. The additional arm increased the stability and had an advantageous effect on the luminescence properties, such as quantum yield and fluorescence lifetime.[17]

Fluorescence polarization (FP) is a tool to follow molecular weight changes. It can be used to study for example enzymatic reactions and molecular interactions, like binding effects, and hydrolysis. The changes in the molecular size can be detected because the binding of the sample compound changes the polarization of the light which is emitted by the fluorescent probe. The measured fluorescence polarization will increase if the fluorescent probe binds to the large particle of interest. When the probe is replaced by a test compound because of the stronger interactions, the measured fluorescence polarization will decrease because the unbound small probe rotates faster when it is free in the solution.[15]

In equation (2) FP is the measured fluorescence polarization and FP_0 is the fundamental polarization, which means the value in the absence of molecular rotation, τ is the lifetime of the excited state of the fluorescence and θ is the rotational correlation time. The rotational correlation time θ can be calculated for a molecule (equation 3). R is the universal gas constant, T is the temperature in Kelvins, η is the viscosity of the solution and V is the molar volume. The fluorescence polarization increases, when θ increases.[15] Based on equation 3, the temperature affects on the measured fluorescence polarization, which means it needs to be optimized carefully and stay stable during the assay. Temperature can also affect some fluorophores' lifetime τ.

$$\frac{1}{FP} - \frac{1}{3} = \left(\frac{1}{FP_0} - \frac{1}{3}\right)\left(1 + \frac{\tau}{\theta}\right) \quad (2)$$

$$\theta = \frac{\eta V}{RT} \quad (3)$$

In fluorescence polarization, the sample with the fluorescent probe is excited with polarized light. The difference between the parallel ($I_{\parallel}$) and perpendicular ($I^{\perp}$) emission intensities normalized by the total intensity is the measured fluorescence polarization (equation 4). It is a ratio of emission intensities and therefore a dimensionless quantity but usually declared in millipolarization units mP, which is FP times gravitational constant G times 1000 (equation 5). G should not be mixed with the grating factor i.e. G-factor in fluorescence polarization. The G-factor is an instrumental setting of the emission optics, and it should be optimized for the assay in question. The G-factor enables the comparison of the results between many instruments without the affect of the sensitivity and performance of an instrument.[15]

$$FP = \frac{I_{\parallel} - I_{\perp}}{I_{\parallel} + I_{\perp}} \quad (4)$$

$$FP(mP) = \frac{(I_{\parallel} - I_{\perp}\, xG)}{(I_{\parallel} + I_{\perp}\, x\, G)} x1000 \quad (5)$$

Some instruments measure the fluorescence anisotropy (FA), which can be converted to fluorescence polarization. Fluorescence anisotropy is the difference in the intensities of the parallel and perpendicular emission which is normalized with the total fluorescence intensity of the sample (equation 6). The conversion to the fluorescence polarization is in equation 7.[15]

$$FA = \frac{I_{\parallel} - I_{\perp}}{I_{\parallel} + 2I_{\perp}} \quad (6)$$

$$FP = \frac{3FA}{2 + FA} \quad (7)$$

The advantage of fluorescence polarization is the one-dye system, no multiple dyes are needed. The advantages of fluorescence polarization are the homogenous format; time-consuming washing steps and separation steps are not needed. FP has also relative insensitivity to interferences and good assay performance i.e. linear range. FP assays' dynamic range is quite constant (free probe compared to bound probe in the solution) because it depends on relative changes in the measurement and not the absolute values.[18] Since FP is a dimensionless ratio, the results are not depending much on the concentration of the fluorescent dye and because of that, low concentrations are able to use. FP assays have relatively low costs and can be read multiple times.[15]

The competitive format with unlabelled target molecules improves the sensitivity of the assay. Fluorescence polarization ImmunoAssays (FPIA) are a specific name for the FP assays which are utilizing antibodies. The rotation of the antibody in the solution is slower when it is bound and therefore the measured FP increases as a function of the concentration of the sample.[15] When compared to other immunoassays, like radioimmunoassays, the FPIAs are easier to be automated for HTS purposes.[19]

1.2.1 The bioimaging of GTP

The imaging of cellular GTP has been done indirectly utilizing various GTP sensors. Recently reported imaging method detects the changes in GTP concentration through a GTP evaluator (GEVALs).[20] The imaging was done with a circularly permuted yellow fluorescent protein (cpYFP, excitation 405/485 nm, emission 530 nm) from living cells. The cpYFP was inserted into a region of G protein (bacterial) which undergoes a GTP-driven change in conformation and therefore the fluorescence emission changes and is proportional to GTP concentration. Two excitation wavelengths were used to measure the ratio of emission to normalize internally the measured GTP, which decreases the emission at ex. 405 nm but increased the emission at ex. 485 nm. The method was tested in the presence of other added nucleotides. Even 500 µM uracil triphosphate (UTP), GMP and CTP did not disrupt the method. The same concentration of inosine triphosphate (ITP) or ATP were disrupting, but they induced less than a 10% change in the measured ratio. The emission ratio was also affected by GDP, but it reduced the change by 10–25% depending on the GDP/GTP ratio (from 1:10 to 10:1, respectively). The cellular GDP concentration is severalfold lower than GTP[12], and therefore less than a 10% change caused by cellular GDP could be expected. The developed method was not able to recognize the difference in the sugar ring between deoxyribose guanosine triphosphate (dGTP) and GTP (ribose), but in the cells GTP concentration is 100-fold higher than dGTP. Mg^{2+} was required for the GTP-driven change in fluorescence emission, but the Mg^{2+} concentration affected the measured fluorescence emission ratio. The emission stayed stable in the cellular concentration range of 0.5–5 mM.[20] The advantage of measuring GTP concentration through GEVALs is the possibility to follow the change as a function of time for hours in living cells. There are limitations of the sensitivity in the imaging through GEVALs since their K_d of binding to GTP is 4–15 µM.[20]

1.3 The development and applications of anti-GTP Fab fragment

In a cell lysate, GTP is a difficult target, since there are similar nucleotides, like GDP and a high concentration of ATP.[12] Therefore a specific binder with high affinity is needed. The novel GTP-specific fragment antigen-binding (Fab fragment) was selected from the designed single-chain variable fragments multipurpose library (ScFvM) with a phage display technique.[21] The affinity of the selected Fab2A4 fragment was over 100-fold higher when compared to similar nucleotides GDP, ATP and CTP. The selected Fab was used to set up a heterogeneous assay for quantitative measurement of GTP. The assay was performed in a 96-well plate coated with anti-mouse immunoglobulin G (IgG) for bound the Fab. In the developed assay, labelled GTP competes for binding to the surface where the Fab is bound and the TRL signal can be measured when labelled GTP is bound. Because of the heterogeneous assay format, washing steps were required to first remove the unbound Fab from the well and second washing step to remove the unbound compounds of the sample matrix. The QRET method was used to monitor the signal of Eu^{3+}-chelate-GTP.[4] The TRL emission at 615 nm of the bound labelled GTP was then measured by using excitation wavelength 340 nm and 400 µs delay and integration times. In the presence of GTP in the sample, the measured TRL signal is low. The optimal final concentration of the GTP binder for the assays was 0–200 nM.[21]

The application of anti-GTP Fab2A4 was developed further and used to study the GTPase cycle.[22] Parameters of the buffer such as salt concentration would affect the affinity of the Fab2A4.[21] Taken into account that, the assay buffer was optimized for the competitive GTP assay. The selected assay buffer was 20 mM hydroxyethyl-piperazine-ethane sulfonic acid (HEPES) pH 7.5, 1 mM NaCl, 1 mM $MgCl_2$, 0.01% Triton X-100 and 0.005% γ-globulins.[22] The QRET-based single-label detection was performed after 10 min reaction stabilization time by using 2.65 µM of modulator MT2, 7.5 nM of Eu^{3+}-chelate-GTP and 12 nM Fab2A4 in 20 µL final volume in 384-well plate format. The final volume was even able to reduce as low as 10 µL. In the competitive nucleotide titration from 0.1 nM to 1 mM the Fab2A4 was monitored to have over 200-fold GTP specificity over ATP, GDP, GMP or guanosine.[22]

1.4 Other assays to measure GTP

GTP can be monitored for example with fluorescence polarization. One main application for FP is to identify the activity of small molecule modulators by measuring the end product of an

enzymatic reaction.[15] For example, nucleotides and the enzymatic hydrolysis of nucleotides can be studied with the commercial Transcreener® FP -assay by BellBrook Lab. The general Transcreener® method is created at least for GDP, ADP and UDP nucleotides. In the assay, the GTPase enzyme converts GTP to GDP by hydrolysis of one phosphate group from the nucleotide (Figure 3). Then GDP binds to a specific antibody and replaces the fluorophore labelled GDP (competitive assay). The dye used is Alexa Fluor 633[23] which can be monitored in the far-red range (ex. 632 nm, em. 647 nm).[24] The fluorescence signal is stable for up to 8 hours. The labelled GDP probe can be used at 2 nM concentration in the final volume of 20 µL. FP measurement can be carried out in 384- and 1536-format with a plate reader.[23] The Z' factor of the assay is over 0.7 at the low conversion of the substrate. The linear range of GTP concentration is 1–1 000 µM.[25] The benefits of Transgreener assay are the low consumption of the detection solution and the long stability of the fluorescence emission but there are limitations in suitable applications reduced only to those enzymes which are converting GTP to GDP. There is also Transcreener® (BellBrook Lab) method based on Time-Resolved Förster Resonance Energy Transfer (TR-FRET) utilizing the same GDP-specific antibody. In TR-FRET the GDP antibody is conjugated with terbium. There is energy transfer between terbium and HiLyte647 (far-red tracer) labelled GDP. GDP of the sample and labelled GDP competes on binding to the antibody. When the GDP of the sample binds to the antibody, the energy transfer does not occur and the detected signal in the far-red range is low.[25]

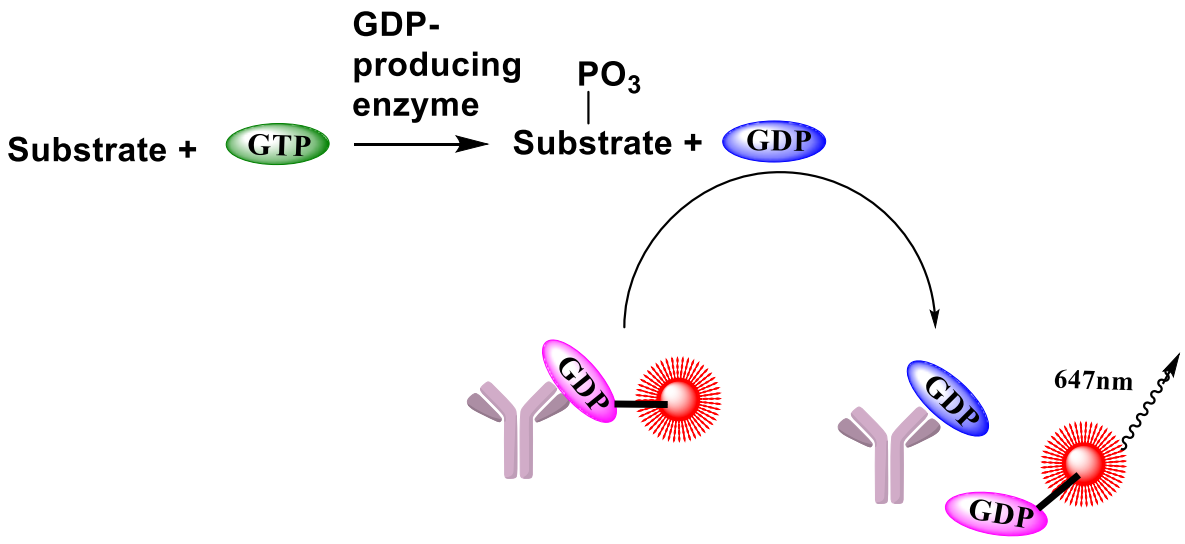

Figure 3. Direct detection of GDP to measure GTPase enzymatic activity with fluorescence polarization. The figure is adapted from manufacturer BellBrook Labs (https://www.bellbrooklabs.com/products/transcreener-hts-assays/gdp-gtpase-assays/gdp-assay-fp/).

As a similar application of FPIA, the novel Fab2A4 fragment is applicable to measure GTP with FP in competitive assay format, where the GTP of the sample and the fluorophore

labelled GTP are trying to bind to the anti-GTP Fab2A4. If there is GTP in the sample solution, the fluorophore labelled GTP probe is not binding because of the competition and the measured FP is lower because the probe rotates faster. If there is not GTP in the sample solution, the Fab2A4 binds with the GTP probe and the measured FP increases. An uncompetitive assay utilizing anti-GTP Fab would be also possible to develop. If the Fab2A4 would be labelled with a fluorophore, the measured FP would increase as a function of the concentration. When compared to the antibodies used in FPIA, the size Fab-fragment is small. Because of the small size of the Fab-fragment, the relative change in weight is significant when the GTP of the sample binds and therefore simple to measure with FP with high sensitivity when compared to the antibody, in which the binding of GTP does not affect as significant relative change in weight. The advantages of competitive or uncompetitive GTP FP assay are, that FP is a general and widely known method and it can be carried out with basic plate readers and does not require time-resolved settings like QRET with lanthanide chelates, because the emission of the fluorescent dye is more direct to measure. On the other hand, this reduces the sensitivity of the assay. In addition, the detection of FP assay implemented in either way does not rely on signal quenching, like in QRET measurement. To avoid the quenching of the signal because of the interactions in the solution, the detection solution must be done each time before use. The detection solution for FP could be a ready-to-use kit, which could be a more easily commercializable tool for Fab2A4 when compared to a QRET assay for GTP. However, this would have novelty value, as current commercial FP assays for GTP do not measure GTP directly, but rather a reaction through GDP and enzymatic reactions of GTP, which are therefore more suitable for biochemical assays with pure sample matrix, and pure enzymes and GDP for example to study the functionality of enzymes. Direct GTP measurement would be important for the fixed cell-based samples to get *in vivo* information of the nucleotides.

1.4.1 Detection of GTP through its hydrolysis

The detection of GTP can be done through the measurement of the free phosphate groups released by GTP hydrolysis. Malachite Green phosphate assay is a colorimetric method to detect phosphate groups in a homogeneous “mix-and-measure” assay format. It can be used in the quantification of free phosphates or steady-state kinetics. The GTP can be detected through its hydrolysis and release of the third phosphate group.[26] The Malachite Green ([4-[[4-(dimethylamino)phenyl]-phenylmethylidene]cyclohexa-2,5-dien-1-ylidene]-dimethylazanium; chloride) is a basic triphenylic dye used in histological staining.[27] The

Malachite Green phosphate assay kit is a commercial kit, which can be used to detect the concentrations of phosphate groups or triphosphates with a plate reader. The quantification is based on the green complex formed between free orthophosphate, molybdate and the Malachite Green dye. The colorimetric assay is based on the colour change from yellow-brown to green when pH decreases, for example when GTP degrades and the amount of free phosphate groups increases in the solution. After 30 min incubation time, the colour formation caused by the reaction can be monitored with a spectrophotometer or a plate reader at the absorbance wavelength 600–660 nm (620 nm). Respectively, Malachite Green assay can be executed in cuvettes or 96- and 384-well plates with the observed Z' factors of 0.7–0.9. The limit of detection is 1.6 pmol and the optimal range is 0.02–40 µM in the final volume of 50 µL (384-plate). The benefits of Malachite green assay are the homogenous format and the stability of the dye and its absorbance signal. It can be used for phosphate determination for a wide range of biological samples.[26] GTP can be measured through its hydrolysis also by a fluorescently labelled phosphate-binding protein (PBP).[28] Binding of a phosphate group changes the conformation of PBP which leads to an increment of the fluorescence emission of the fluorophore. The conjugated fluorophore is N-[2-(1-maleimidyl)ethyl]-7-(diethylamino)coumarin-3-carboxamide and the conformational change of PBP increases fluorescence 7-fold higher. The advantage of PBP is that it can be used for real-time monitoring of phosphate production for example in GTP hydrolysis. The use of PBP is simple and assays are quick to perform. PBP is very stable when conjugated with the fluorophore. The limitations of these two methods are the indirect detection of GTP through the released phosphate group and therefore also a high contamination risk due to the enzymes and free phosphate groups in the environment.[28]

1.4.2 Bioluminescent techniques

Glo (Promega Corporation) is a homogeneous method based on bioluminescence.[29] The GTPase-Glo can be used to measure the activity of GTPases by monitoring the amount of GTP after a GTPase reaction.[30] GTP is converted to ATP which can be detected using luciferase and luciferin substrate to produce luminescence emission. Luciferase is a monomeric enzyme which catalyses an oxidation of luciferin. First, the ATP is required for activation of the protein to produce an anhydride intermediate which then reacts with oxygen to a transient dioxetane. The dioxetane breaks down fast to oxyluciferin and carbon dioxide and emits light at 560 nm.[31] This luminescence can be detected with a chemiluminometric microplate reader, and it is proportional to the concentration of ATP when ATP is the limiting

reagent. The emission is inversely proportional to the activity of GTPase since active GTPase hydrolyses more GTP than inactive. A less active GTPases hydrolyses less GTP and therefore more GTP is converted to ATP leading to a higher emission signal. The GTPase-Glo can be used in 96- and 384-format in respective final volumes of 100 or 20 µL.[30]

1.4.3 Separation-based techniques

In the past, the nucleotide concentrations have been mostly measured with chromatographic[12] and mass spectrometric methods.[32] High-Performance Liquid Chromatography (HPLC) is a separation method which is based on the interactions between the components in the stationary phase of the column and the eluent. The chemical structure, charge or molecular weight of the compounds leads to different retention times.[33] GTP and other nucleotides are usually separated by basic reversed-phase liquid chromatography (RPLC) or anion exchange chromatography techniques and can be detected with an ultraviolet (UV) detector.[1] In RPLC the separation is based on the different adsorption of the polar compounds. The stationary phase consists of SiO_2 particles with nonpolar hydrocarbon chains (for example C_8, C_{18}).[1,33] Polar compounds have the weakest interaction with the stationary phase and elute first. The polarity of the compounds decreases as a function of retention time.[33] The retention order of the nucleotides is monophosphates, diphosphates and triphosphates at low pH. The retention order depends on the overall size of the molecule and the number of phosphate groups, which interact with the stationary phase.[1] The substituents of the nucleobase and their position affects the retention time as well (elution order OH, H, NH_2, NHR).[1] In anion exchange chromatography, the stationary phase is positively charged, for example by ammonium or amine groups. Because of the phosphate groups, nucleotides are negatively charged at physiological pH. Most negatively charged molecules interact strongest with the stationary phase and elute and therefore nucleotide monophosphates and diphosphates can be separated from triphosphates.[1]

Another widely used detector is mass spectrometry (MS). The MS techniques used for nucleotides can be for example ion trap (IT)[21,32] or matrix-assisted laser desorption ionization (MALDI).[34] In the IT detector the ions are trapped and circulate between electrodes until a voltage is applied to the one electrode and changed systematically to obtain the entire mass spectrum. Ions with specific m/z values are directed towards the detector due to the alternating voltage. In the IT-MS method example, the sample size was 50 µL and the retention time of GTP was 20.08 min. The achieved limit of quantification was 50 nM but the

required cell number was high (5-6x10^6 cells). The detected M-H^- ion m/z was 424.0 because of the phosphate cleavage from the original GTP (m/z 522.3). The coefficient of variation (CV%) for the method of GTP was 13.3% (n=5).[32] MALDI can be used for relatively large compounds. Laser pulses are used for ionization in MALDI. In the MALDI-MS method created, the sample size was 0.5 µL and concentration as low as 50 pmol were able to detect from the cell sample matrix.[34]

Capillary electrophoresis (CE) has been used to detection of nucleotide monophosphate, diphosphate and triphosphate.[35] In CE, silica-filled or otherwise coated capillaries are used for separation under an electric field. In the CE method example, the nucleotide analytes were separated in silica capillary under 28 kV voltage for 6 min and monitored with a diode-array detector at the wavelength 254 nm. The GTP concentration range utilized was 0.5-4 mM and the method may also be applied to the analysis of other nucleotides.[35] CE can also be combined with mass spectrometry (CE-MS).

The advantages of these separation-based methods are the simultaneous measurement of many different nucleotides. They are also widely used and traditional methods. These methods lack the ability to be performed with a high number of samples with low intracellular concentrations. The long preparation and separation times expose the labile triphosphates for hydrolysis, which is a source of error and these measurements can not separate between the free and total nucleotide concentrations. The free GTP levels possibly differ from the total concentration.[5] Separation-based techniques require a lot of instrumentation and methods have many complicated steps. The consumption of solvents is high and the number of samples is limited, which reduces also the number of replicates.[28] The choice of technique depends on factors such as the specific analytical goal, the sample matrix, and the desired sensitivity and resolution.

1.5 The aim of the work

The goal of this Thesis work was to be able to monitor the exact GTP level in differently treated cells. The aim was to develop methods for direct GTP measurement by utilizing the novel GTP-specific Fab fragment. The developed anti-GTP Fab fragment has a high potential to be utilized in various applications. In the past, the imaging of free GTP has been indirect and utilized by sensors through a GTP-driven conformational change. In this work, the method was developed to be able to use the anti-GTP Fab fragment as a primary antibody in immunofluorescence from the fixed U87MG (or HeLa) cells and therefore directly image the

changes in the GTP level. The GTP concentration from the GTP biosynthesis deficient DKO cells and WT cells are monitored in various conditions and after co-culture. In multicolour immunostaining, IMPDH2 was also stained to confirm the changes caused by the treatments and to study the affect of treatments on GTP-synthetic IMPDH2 enzyme and GTP simultaneously.

Intracellular nucleotides are difficult targets for imaging from fixed cells and require specific binders with high affinity. Additionally, the high intracellular ATP concentration sets high demands for GTP binder specificity. The ideal probe should be selective to the triphosphate form and also to the right nucleobase in question. It is also required for the probe to be capable insert the cell membrane and be also stable in the staining conditions. The novel anti-GTP Fab fragment would fulfil the requirements and is a promising candidate for the imaging of GTP.

The aim of the GTP-ATP assay was to measure the concentrations of the free GTP and ATP directly from the cell lysate. This homogenous assay is utilizing anti-GTP Fab2A4. This kind of assay for direct GTP concentration monitoring would be needed in the field of basic cancer research since there has been a lack of direct techniques. When combined with a commercial ATP kit, the ATP-GTP ratios can be studied, giving more information about the energetic state of the cells. The ATP concentration can be used as an internal standard for GTP since the ATP per cell remains stable. The concentrations from the GTP biosynthesis deficient DKO cells and WT cells are monitored in various conditions and after co-culture. There is a high possibility to convert the new information to the development of new drugs.

2 Materials and methods

2.1 Cell culture

HeLa WT (cervical cancer, ATCC line), U87MG WT (glioblastoma, ATCC line) and U87MG IMPDH1/2-DKO [9] cells were used. The glass slides in 24-well plates (BioLite 24-well multidish, ThermoScientific, Korea) were coated with 0.01% poly-L-lysine-solution (PLL-solution, Sigma-Aldrich) for 1 h and then the wells were washed three times for 1 h with sterile MilliQ-water (MQ). The cells were cultured either on the coated glass slide ($0.5x10^5$ cells in each well) or on the 4-chamber glass slides ($1x10^6$ U87MG WT cells or DKO cells $7x10^4$ in each chamber) for immunofluorescence imaging.

On the BioLite 48-well plate (ThermoScientific) the U87MG WT and DKO cells were inoculated ($4x10^4$ cells in each well) for the crystal violet assay. For the GTP-ATP assay, the U87MG WT and DKO cells were cultured on the 10 cm dish (100 mm TC-treated culture dish, Corning, NY, USA) or the 6-well plate (Tissue Culture Plate, 6 wells, Fisherbrand) or on the T75-flask (Corning).

U87MG IMPDH1/2-DKO cells were also co-cultured with U87MG WT or U87MG IMPDH1/2-DKO cells. The plate used was a 24-well tissue culture plate with polyethylene terephthalate (PET) membrane –inserts, with the pore size of 1.0 or 8.0 µm (VWR, China). The DKO cells were inoculated on the PLL-coated glass slide and the WT or DKO cells on the PET membrane ($0.5x10^5$ cells in each well or insert) and co-cultured for 12–48 h for further use in the immunofluorescence. For the GTP-ATP assay, the co-culture plate used was a 6-well tissue culture plate with PET membrane -inserts, with the pore size of 1.0 µm (VWR) or 3.0 µm (Corning Incorporated Costar Transwell, ME, USA). The DKO cells were inoculated in the well and the WT cells or DKO cells on the PET membrane ($5x10^5$ cells in each well or insert) and co-cultured for 12–72 h.

The culture conditions in the incubator were 37 °C and 5.1% CO_2. The culture medium was high glucose DMEM (Dulbecco's Modified Eagle Medium) (Cytiva, HyClone, UT, USA or Nacalai Tesque Inc., Japan or Life Technologies Limited, Gibco, UK) supplemented with 10% serum (FetalPlex, Gemini bioproducts, animal serum complex, USA or Fetal Bovine Serum (FBS), Gibco, UK), 1xPenicillin-Streptomycin solution (Cytiva, UT, USA or Corning, VA, USA or Gibco, Life Technologies Limited, UK), and 0.07% Plasmocin prophylactic (InvivoGen, CA, USA) or 0.07% Normocin 50 mg/mL (InvivoGen) against mycoplasma.

2.2 The treatments for the cells

Cultured HeLa (17 or 23 h) and U87MG WT cells (15 or 20 h) were washed with phosphate-buffered saline (1xPBS) and treated with 0.1% dimethyl sulfoxide (DMSO), 10 µM MPA, 100 µM guanosine or 10 µM MPA + 100 µM guanosine -medium. The treatment time was 8 h for the HeLa cells and for the U87MG WT 5 h, 6 h, 26 h or 33 h depending on the sample. The co-cultured (48 h) DKO cells were treated with 10 µM MPA medium for 4 h. After the treatment the cells were washed twice (1xPBS) and used for the immunofluorescence

Cultured (24 h) U87MG WT cells on the 48-well plate were first treated with 0.1% DMSO or 10 µM MPA. After the treatment (8 h) the medium was replaced with fresh 10 µM MPA medium or the rescue medium for 12–92 h and then used for the crystal violet assay. The rescue mediums were 0.1% DMSO, 50 µM or 100 µM guanosine medium or medium from separate cultures, which were induced with 0.1% DMSO, 50 µM guanosine or 100 µM guanosine for 8 h.

The cultured (2–150 h) U87MG WT and DKO cells were washed with 1xPBS and treated with 0.1% DMSO, 10 µM MPA, 50 µM or 100 µM guanosine or 50 µM GTP. After the treatment (2–150 h) cells were washed twice (1xPBS) and used for the GTP-ATP assay.

2.3 Immunofluorescence

The cells for immunofluorescence were fixed by adding 4% paraformaldehyde (PFA) in 1xPBS (ThermoScientific, USA) for 10 min at room temperature (RT). After washing the cells three times with 1xPBS, the plates were stored at 4 °C with 1xPBS (1–7 days) or 1xPBS with 0.1% Tween20 (Research Products International, USA) (7–34 days) in the wells. The U87MG WT and DKO cells on the chamber glass slide were stained immediately after fixation.

Before permeabilization, the cells were washed 3 times with cold 1xPBS, for 5 min each wash. The permeabilization of the cells was done with 0.5% saponin in 1xPBS for 10 min at RT. For the U87MG WT and DKO cells on the chamber glass slides the permeabilization of the cells was done with 0.2% Triton X-100 in 1xPBS for 10 min at RT. Then the cells were washed 3 times with cold 1xPBS with 0.1% Tween20 (1xPBS-T) or 1xPBS, for 5 min each wash. The cells were incubated in 10% goat serum (Gibco) in 1xPBS-T for 30 min at RT to block the unspecific binding of the antibodies. The blocking step for U87MG WT and DKO

on the chamber glass slide was done with 1% bovine serum albumin (BSA) in 1xPBS-T for 60 min at RT.

The immunostaining started by adding the primary antibody to the wells in 1% BSA in 1xPBS-T or 1xTBS-T and incubated overnight at 4 °C in humid conditions. The primary antibodies used were mAb anti-IMPDH2 (Abcam, 2b131158 rabbit mAb, 0.134 mg/mL), anti-GTP fragment antigen-binding (Fab2A4)[21] or maturated anti-GTP-Fab (Fab2A4m). The wells were washed 3 times with cold 1xPBS-T or 1xTBS-T, for 5 min each wash. The cells were incubated with the fluorescently labelled (AlexaFluor, ThermoFisher Scientific or FITC, Sigma Aldrich) secondary antibody (Table 1) in 1% BSA in 1xPBS-T or Tris-buffered saline (1xTBS-T) for 1 h at RT and protected from light. The combinations of primary and secondary antibodies which were tested are in Table 1. The wells were washed 3 times with cold 1xPBS-T or 1xTBS-T for 5 min each wash.

Table 1. The primary and secondary antibodies.

1st antibody	2nd antibody	Dye	Absorption max. (nm)[24]	Emission max.(nm)[24]	Colour
rabbit IgG anti-IMPDH2 Ab	goat anti-rabbit IgG	AlexaFluor488	495	519	Green
		AlexaFluor568	578	603	Red-orange
anti-GTP Fab2A4	goat anti-mouse IgG	AlexaFluor488	495	519	Green
		AlexaFluor568	578	603	Red-orange
	goat anti-mouse IgM	AlexaFluor488	495	519	Green
	Fab-specific goat anti-mouse IgG	FITC	495	521	Green
anti-GTP Fab2A4m	goat anti-mouse IgG	AlexaFluor488	495	519	Green

In multicolour immunostaining, the U87MG cells were incubated simultaneously with both primary antibodies overnight at 4 °C in humid conditions (anti-IMPDH2 mAb with 1%BSA and either Fab2A4 in 1xTBS-T or Fab2A4m in 1xPBS-T). The cells were washed 3 times with cold 1xTBS-T or 1xPBS-T, for 5 min each wash. Then simultaneous incubation with the respective secondary antibodies with 1% BSA at RT and protected from light: goat-anti-rabbit IgG AlexaFluor568 (AF568) and Fab-specific goat anti-mouse IgG FITC for Fab2A4 in 1xTBS-T for 1 h or goat-anti-mouse IgG AlexaFluor488 (AF488) for Fab2A4m in 1xPBS-T for 2 h. The cells were washed 3 times with cold 1xTBS-T or 1xPBS-T, for 5 min each wash.

The nuclei staining was performed by using 1:2000 diluted Hoechst 33342 (Thermo Fisher Scientific) in 1xTBS-T. The cells were incubated for 1 to 5 min with Hoechst and then rinsed with cold 1xTBS-T. 10 µL of Fluoromount-G (SouthernBiotech) viscose liquid for mounting was added to the glass slide. The cover glass with the cells was transferred from the 24-well upside-down on the dropped Fluoromount-G. The sample was left to dry at RT (for 3 h to 4 days) and protected from light. With the U87MG WT and DKO cells on the chamber glass slide, nuclei staining and mounting were done in the same step. After multicolour immunostaining, the walls of the chambers were removed from the glass slide. Nuclei staining and sample preparation were done simultaneously by adding Fluoromount-G with DAPI, one droplet in each chamber's area. The cover glass was added, and air bubbles were removed carefully. The sample was left to dry at RT for 2 h in the dark protected from light. The fluorescence microscopy (Keyence BioRevo BZ-9000 fluorescence microscope, Keyence, Osaka, Japan and the BZ II viewer software) was used for observing the immunofluorescence samples with the respective wavelengths of the dyes (Table 1). The lens used were a 60x oil lens and a 40x lens.

2.4 Crystal violet

The cultured U87MG WT cells (8 h and 12–92 h rescue) were fixed by adding 4% PFA in 1xPBS (ThermoScientific) for 10–15 min at RT. Then the wells were rinsed with washing buffer (0.1% BSA in DMEM). The cells were stained with 0.2% crystal violet solution in 2% EtOH for 10 min at RT and then the wells were washed 3 times by decanting gently with tap water and left to dry at RT. After 1–3 days, the 2% SDS- detergent solution was added to the wells and the plate was shaken for 30 s on the plate shaker. The absorbance of the wells was measured by a plate reader (λ=590 nm). The absorbance is proportional to the proliferation rate of the cells. The samples (triplicate) signal's average µ and standard deviation σ were calculated in Excel (Microsoft, USA) and the measurement data was analysed with Origin 8 v2016 (OriginLab, MA, USA).

2.5 Labelling and purification of the GTP with the 9-dentate Eu^{3+}-chelate

9-dentate Eu^{3+}-chelate 4-[2-(4-isothiocyanatophenyl)ethynyl]-2,6,-bis{[N,Nbis(carboxymethyl)-amino]methyl}pyridine europium(III), bearing one additional iminodiacetate coordinating arm[17] was synthesized and conjugated with GTP based on previous publications.[21,22] 50 mM carbonate buffer (Na_2CO_3, $NaHCO_3$) was prepared and the

pH was 9.8. 9-dentate Eu^{3+}-chelate (QRET Technologies, Finland) with the iminodiacetate reactive arm was dissolved in 50 µL MQ water. 10 mM 2'- / 3'- O- (6-aminohexylcarbamoyl)guanosine- 5'- O- triphosphate's sodium salt (2'-/3'-AHC-GTP, pH 7.6) (BIOLOG Life Science Institute, Germany) was labelled covalently with dissolved Eu^{3+}-chelate. The final volume of Eu^{3+}-GTP-chelate was 150 µL, in which the carbonate concentration was 50 mM. The conjugation reaction was protected from light and left overnight at RT.

Dionex UltiMate 3000-HPLC system (Thermo Fisher Scientific) was used to purify 9-dentate Eu^{3+}-chelate-GTP. The column used was Ascentis RP-Amide C18 15 cm x 4.6 mm, 5 µm (Supelco Analytical, Cat. 565324-U, Sigma-Aldrich, MO, USA). Diluted the Eu^{3+}-chelate and labelled GTP in 50 mM triethylammonium acetate buffer (TEAA) pH 7.0 (PanReac AppliChem ITW Reagents, Germany) and injected it into the column. The purification of the 9-dentate Eu^{3+}-chelate-GTP was followed with a Dionex Diode Array UV detector (Thermo Fisher Scientific) at the wavelength 280 and 340 nm by using the Chromeleon Chromatography Data System software (Thermo Fisher Scientific). The linear gradient of acetonitrile (ACN, Sigma-Aldrich) increased from 5 to 45% in 30 min and the flow rate was 1 mL/min. The {2,2',2",2'"-{[4'-(4'"-isothiocyanantophenyl)-2,2',6',2"-terpyridine-6,6"-diyl]bis(methyleneinitrilo)}tetrakis(acetato)}europium(III) (QRET Technologies, Finland) labelled GTP was prepared and purified similarly earlier.

The fractions were dried in the concentrator overnight in a vacuum and then dissolved in 50% dimethylformamide (DMF). The binding properties of the Eu^{3+}-chelate-GTP samples were tested with the anti-GTP Fab2A4 of the GTP assay to select the fractions. The concentrations of the selected Eu^{3+}-chelate-GTP fractions were determined based on the Eu^{3+}-ion concentration by comparing the measured TRL signals with standard (1 nM Eu^{3+} from $EuCl_3$) in the Delfia assay system in the well plate (C12 low fluor maxi, bright, Thermo Fischer Scientific, Nunc, Denmark) in duplicate in 200 µL volume. The plate was protected from light and after 10 min incubation time the TRL signals were monitored with Tecan Spark 20M plate reader (Tecan Life Sciences, Männedorf, Switzerland). The excitation wavelength was 340 nm (± 35 nm, filter) and the measured emission wavelength was 620 nm (±35 nm, filter). The lag time between excitation and emission was 400 µs and the integration time of the measurement was 400 µs. Then the original concentrations of the samples were calculated.

2.6 GTP-ATP assay

The cells for the GTP-ATP assay were detached with 0.25% Trypsin + 2.21 mM EDTA (Corning, VA, USA) and the plate was incubated for 5 min (37 °C, 5.1% CO_2). The cell detachment was suspended in the medium and the suspension was collected in the centrifuge tube. The tube was centrifuged at 110–300g for 5 min and the supernatant was discarded. The cell pellet was washed twice with 1xPBS and centrifugation. The aliquot for cell counting was collected and then the cells were centrifuged again at 110–300g for 5 min. The cell count was done manually with the cell count chamber or with Countess II FL automated cell counter (ThermoFisher Scientific). The cell lysis and precipitation of nucleotides was done by suspending the cell pellet in 500–1 000 µL of 80% methanol (MeOH) in 1xPBS. The tube was centrifuged at 1735–5000g for 5 min to remove solid macromolecules. The supernatant was collected and stored at – 80 °C. The cell-based samples (the precipitated nucleotides in the methanol) were stored for 2–80 days at – 80 °C.

The cell-derived samples in 80% methanol (including the nucleotides) were diluted with the assay buffer (25 mM hydroxyethyl-piperazine-ethane sulfonic acid (HEPES) pH 7.5 (Gibco, Life Technologies, UK), 10 mM NaCl, 1 mM $MgCl_2$, 0.01% Triton X-100). GTP and ATP concentrations were determined against the known standard solutions. The standard curve with pure GTP and ATP was prepared into the assay buffer with 15% methanol. The methanol was added to ensure similar background signals with the cell-based samples. The cell-based sample dilutions and standards were added to the white 384-well plate (Corning 384-well Low Volume White Round Bottom Polystyrene, ME, USA) in triplicate at 5 µL volume. The detection solution for the GTP assay consists of three components in the assay buffer and the detection solution was prepared into a microcentrifuge tube. Detection of GTP was performed by using 20 nM anti-GTP 2A4Fab, 10 nM Eu^{3+} -chelate GTP, 2.7 µM soluble MT2 quencher (used according to the manufacturer's instruction, QRET Technologies, Finland), in a 10 µL final volume in the well.[22] The plate was protected from light and incubated for 10 min. The TRL signals were monitored with Spark 20M plate reader. The excitation wavelength was 340 nm (± 35 nm, filter) and the measured emission wavelength was 620 nm (±35 nm, filter). The lag time between excitation and emission was 800 µs and the integration time of the measurement was 400 µs.

10 µL of the ATP Assay kit (ReadiUse™ Rapid Luminometric ATP Assay Kit, AAT Bioquest, USA) was added to the wells and the plate was protected from light. After 10 min

incubation, the luminescence signals (emission 560 nm) were measured (settle time 100 ms, integration time 1 000 ms) with the plate reader from the final volume of 20 µL.

The samples signal's average µ and standard deviation σ were calculated in Excel (Microsoft, USA). The coefficient of variation (CV%) was calculated (σ/µ*100%) to compare the relative error and the signal-to-background (S/B) of the linear range was calculated as μ_{max}/μ_{min}. The standard curves were drawn and the measurement data was analysed with Origin v2016 (OriginLab, MA, USA) by using a "Linear fit" basic plot of the software.

3 Results and discussion

3.1 Immunofluorescence

The aim was to develop a method for bioimaging of cellular GTP by using the anti-GTP Fab fragment as a primary antibody in immunofluorescence. IMPDH2 is a GTP-synthetic enzyme, and its changes after different treatments would indicate the expected changes in detected GTP concentrations in imaging. In multicolour immunostaining, IMPDH2-enzyme was also stained with commercial primary and secondary antibodies. With the developed multicolour immunostaining method, the aim was to compare the differences between U87MG WT and U87MG DKO cells.

In the early steps of the method development, HeLa cells were used instead of U87MG neurons. HeLa cells are highly applicable for fluorescence microscopy because of their rounded shape. The cultured (17–24 h) cells were treated with 0.1% DMSO (negative control for treatments), 10 µM MPA, 100 µM guanosine or 10 µM MPA + 100 µM guanosine. These treatments were selected to cause differences in IMPDH2-enzyme.[10,11] The affect of treatments (Figure 4) was first tested with commercial antibodies, rabbit anti-IMPDH2 Ab as a primary antibody and goat-anti-rabbit IgG AF488 as a secondary antibody. In the MPA-treated cells, the IMPDH2-enzymes seem aggregated (RR effect).[7] As a precursor of GTP, guanosine would increase the activity and the detected signal was bright. With both additives, some aggregation can still be noticed, but the result is in between both additives alone. With both additives, guanosine increases the GTP concentration which inhibits the reversible effect of the MPA treatment. These fluorescence microscopy results indicate that the treatments for the cells were working, and the differences can be detected with commercial antibodies (Figure 4). The treatments cause differences in IMPDH2-enzyme and differences in GTP concentration can be expected. Therefore the same treatments were used in further steps, to cause differences in GTP concentration and confirm if the developed immunostaining method for GTP can detect the differences in GTP level.

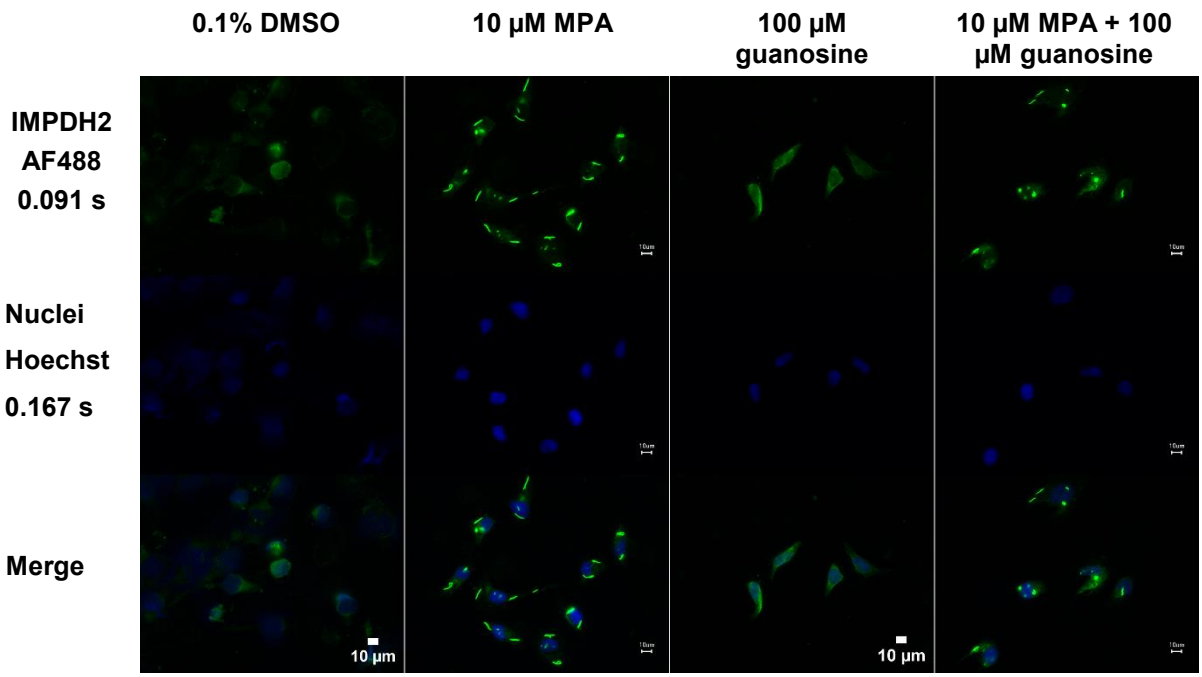

Figure 4. The stained IMPDH2-enzymes of HeLa cells (cultured 17 h) after different treatments (8 h). The primary antibody used was rabbit anti-IMPDH2 (1:400) and the secondary antibody was goat-anti-rabbit IgG AF488 (1:250). The scale bar is 10 µm and the exposure times were 0.091 s for AF488 and 0.167 s for Hoechst (nuclei).

The bioimaging of GTP with anti-GTP Fab fragment as a primary antibody requires a suitable fluorescent secondary antibody in optimal dilution. Based on preliminary data (not shown), an anti-GTP Fab fragment was used with goat-anti-mouse IgG AF488 as a secondary antibody. First, the background signal of the cells and the unspecific binding of the secondary antibody were tested, the negative controls without the primary antibody and with the secondary antibody in dilutions 1:250 or 1:500 are in the Figure 5. With higher secondary antibody concentration (1:250), the detected fluorescence was high because of the unspecific binding than with lower concentration. Based on this, the lower concentrations (1:500) of the secondary antibody would have been optimal to reduce the signal of the unspecific binding.

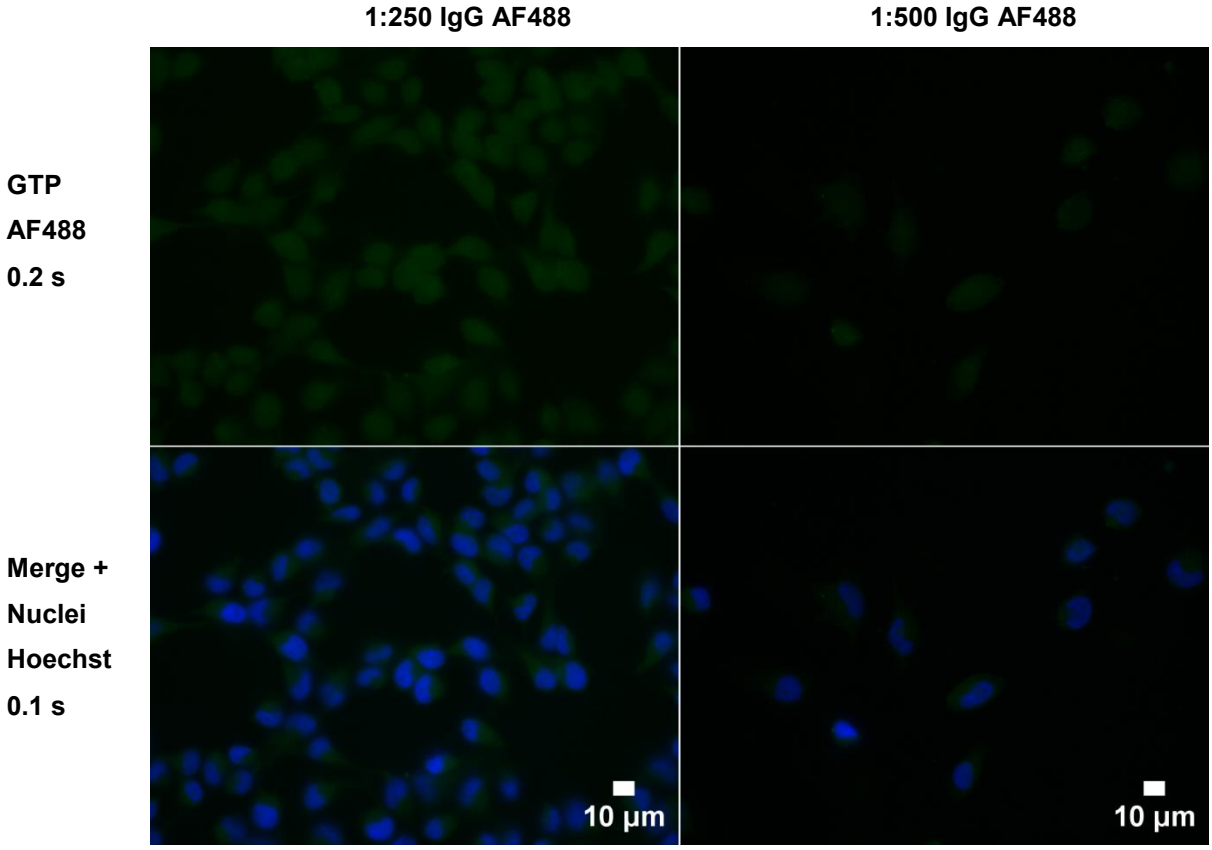

Figure 5. Negative controls of the cultured (24 h) and treated (DMSO, 8 h) HeLa cells. No primary anti-GTP antibody, only secondary antibody IgG AF488 was added in 2 dilutions (1:250 and 1:500). The scale bar is 10 µm and the exposure times were 0.2 s for AF488 and 0.1 s for Hoechst (nuclei).

For the primary antibody the concentrations of 6–420 nM were used with Fab2A4 (Figure 6) and 1.5–60 nM were used with maturated Fab2A4m (Figure 7). The secondary antibody concentration was high (1:250) and a significant part of the fluorescence in all the samples is caused by the unspecific binding of the secondary antibody. With the Fab2A4m concentration of 1.5 nM, the detected fluorescence is at a similar level with both samples, control cells (DMSO) and guanosine-treated cells. With the 6 nM Fab2A4 the detected fluorescence was low despite the longer exposure time (0.357 s) used. Concentrations 1.5 nM and 6 nM were too low for use, because with these low concentrations the differences between the treatments could not be confirmed. On the other hand, the concentration of 420 nM was unreasonably high for use. The detected fluorescence level can also be adjusted by the exposure times. With the same exposure time, the detected fluorescence is lower with 20 nM when compared to 210 nM and 420 nM. Lower antibody concentrations are more cost-effective and therefore it is beneficial to adjust the exposure time for lower concentrations. The differences between the treatments were detected with Fab2A4m at the concentration of 60 nM: the fluorescence is brighter in guanosine-treated cells when compared to the control cells (DMSO). Based on these results the concentrations of 20 nM and 210 nM for Fab2A4 and 60 nM for Fab2A4m were selected for further use in optimisation tests.

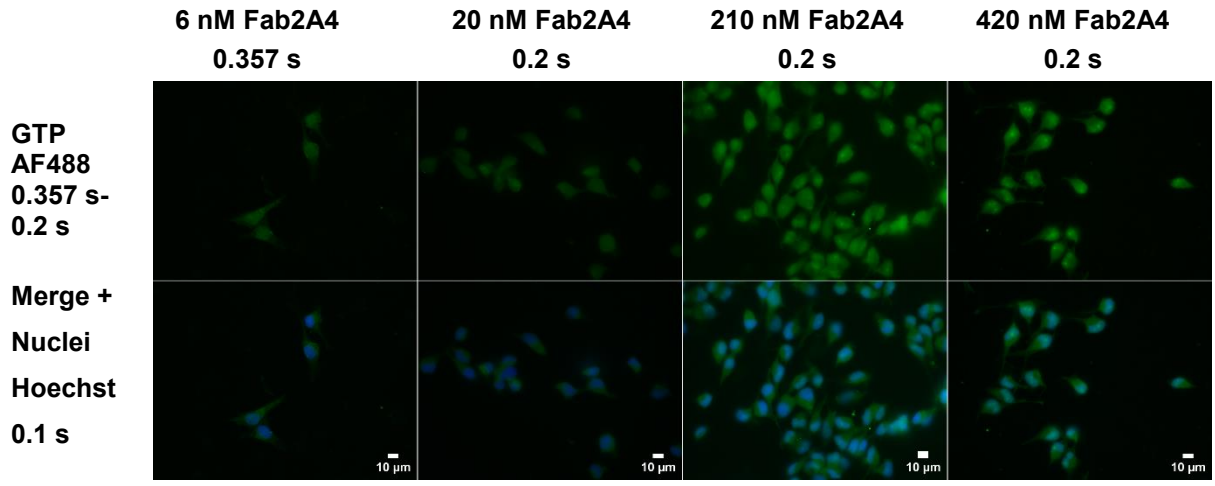

Figure 6. The comparison of different primary antibody Fab2A4 concentrations (6, 20, 210, 420 nM). The secondary antibody IgG AF488 dilution stays constant (1:250). HeLa cells were cultured for 24 h and then treated for 8 h, only the results of the treatments with 0.1% DMSO are shown. The scale bar is 10 µm and the exposure time for AF488 was 0.357 s (6 nM) or 0.2 s and for Hoechst (nuclei) 0.1 s.

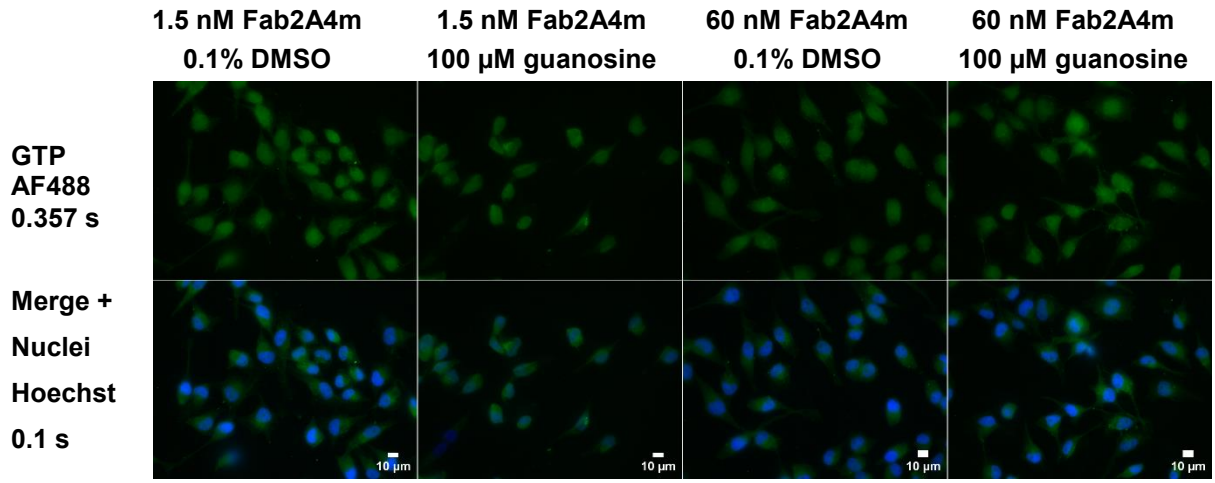

Figure 7. The comparison of different primary antibody Fab2A4m concentrations (1.5 nM and 60 nM). The secondary antibody IgG AF488 dilution stays constant (1:250). The HeLa cells were cultured for 24 h and then treated for 8 h. The results of the treatments with 0.1% DMSO (control) and 100 µM guanosine are shown. The scale bar is 10 µm and the exposure times were 0.357 s for AF488 and 0.1 s for Hoechst (nuclei).

With 20 nM and 210 nM Fab2A4, three different dilutions (1:250, 1:500 and 1:1000) of the secondary antibody IgG AF488 were tested to optimize the concentrations (Figure 8). The washing steps after the addition of the antibodies was done with 1xTBS-T or 1xPBS (the third column in Figure 8). The change from PBS to TBS was done to decrease the background signal which was higher with PBS washes (the third column in Figure 8) and to protect the Fab fragment from the high salt concentration. With 20 nM Fab2A4, the detected fluorescence is low. With higher concentrations of the antibodies (210 nM Fab2A4 and 1:250 or 1:500 IgG AF488) the detected fluorescence is higher in comparison to other combinations. With the combination of 210 nM Fab2A4 and 1:1000 diluted IgG AF488, the detected fluorescence is similar level when compared to lower Fab2A4 results. For Fab2A4 the concentration of 20 nM is quite low for use and even with higher concentrations, some differences can be detected between the treatments but the sensitivity is poor to show the differences clearly. When comparing to the results of the negative controls, part of the fluorescence with the highest concentration (1:250) was caused by unspecific binding of the secondary antibody. The signal of the unspecific binding is significantly lower with the dilution 1:500. Based on this, the lower secondary antibody concentrations (1:500 and 1:1000) would be more optimal for further use.

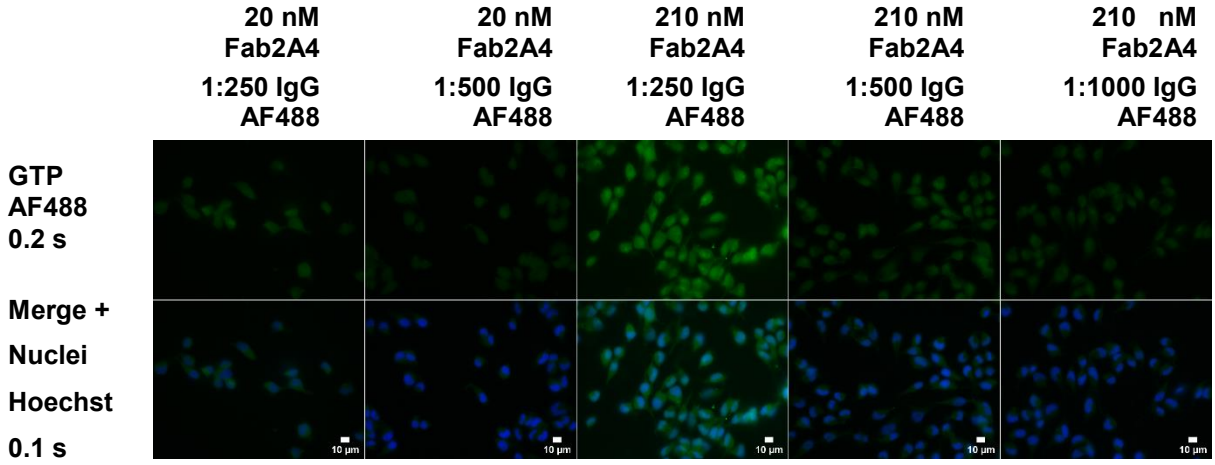

Figure 8. Comparison of different secondary antibody IgG AF488 concentrations with Fab2A4. Three different dilutions of IgG AF488 were used: 1:250, 1:500 and 1:1000. Dilutions 1:250 and 1:500 were tested with two different Fab2A4 concentrations: 20 nM and 210 nM. The HeLa cells were cultured for 24 h and then treated for 8 h. The results of the treatments with 0.1% DMSO (control) are shown. The scale bar is 10 µm and the exposure times were 0.2 s for AF488 and 0.1 s for Hoechst (nuclei).

The detected fluorescence was bright with Fab2A4 at the concentrations of 210 (Figure 9), 230, and 420 nM and Fab2A4m at 60 nM (Figure 10). The used high secondary antibody concentration (1:250) reduces the sensitivity because part of the fluorescence was caused by unspecific binding. Nevertheless, differences between the treatments could be noticed with

these higher antibody concentrations (Figures 9 and 10). The fluorescence was slightly diminished from MPA-treated cells and brighter from guanosine-treated cells when compared to the control sample (DMSO). With Fab2A4m the differences in the fluorescence level were more significant, especially with the guanosine-treated sample. For 60 nM Fab2A4m the used exposure time was longer (0.357 s) when compared to 210 nM Fab2A4 (0.2 s) because of the lower concentration of the Fab2A4m. Based on these results, the Fab2A4m was able to show the possible differences semi-quantitatively between the treatments and it can be used in lower concentrations than Fab2A4.

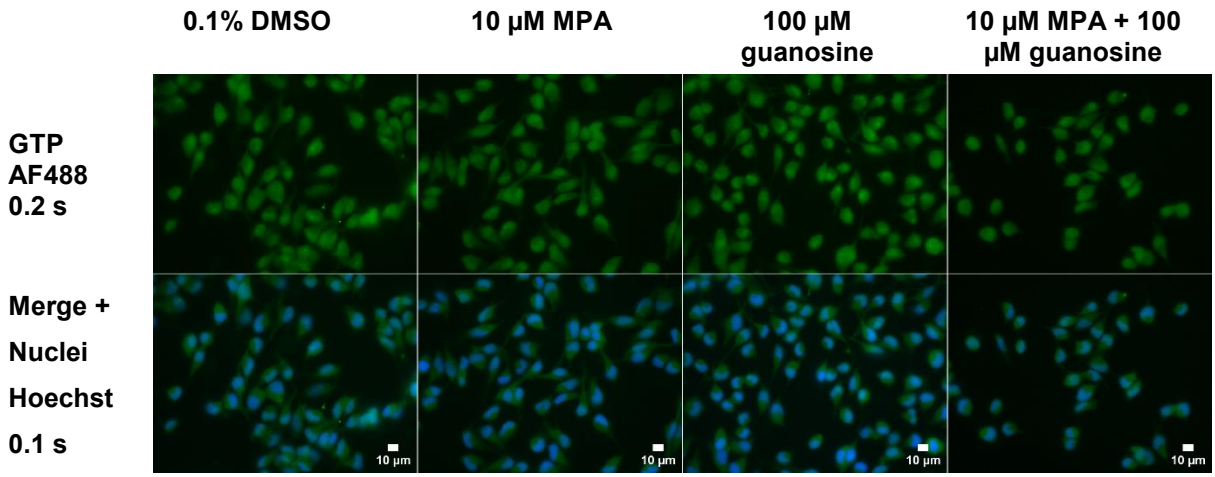

Figure 9. The differences between the treatments can be detected with Fab2A4 in high antibody concentrations (210 nM Fab2A4 + 1:250 IgG AF488). The HeLa cells were cultured for 24 h and then treated for 8 h. The scale bar is 10 µm and the exposure times were 0.2 s for AF488 and 0.1 s for Hoechst (nuclei).

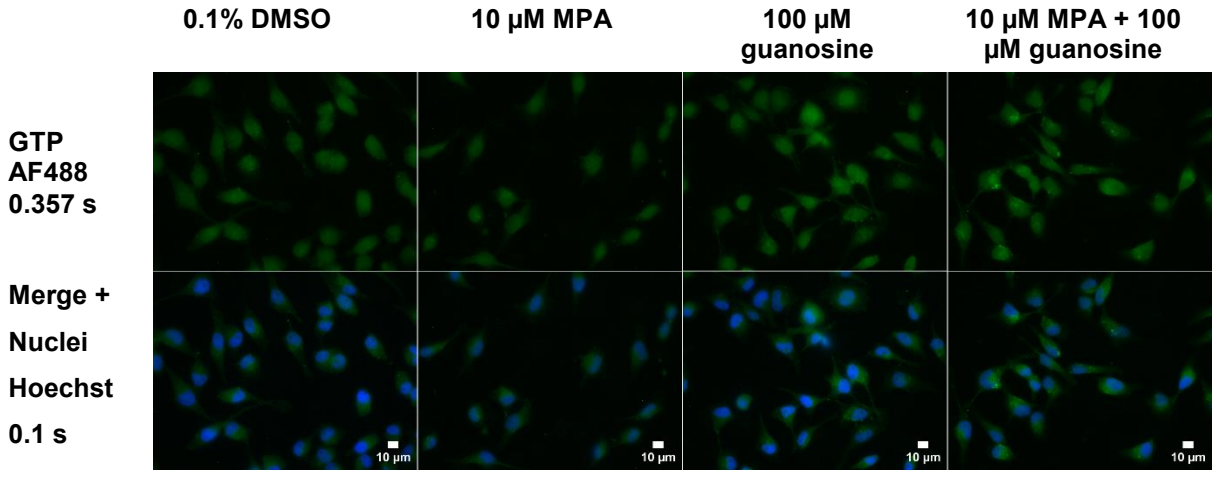

Figure 10. The differences between the treatments can be detected with Fab2A4m in high antibody concentrations (60 nM Fab2A4m + 1:250 IgG AF488). The HeLa cells were cultured for 24 h and then treated for 8 h. The scale bar is 10 µm and the exposure times were 0.357 s for AF488 and 0.1 s for Hoechst (nuclei).

In addition to goat-anti-mouse IgG AF488, three secondary antibodies were tested: goat-anti-mouse IgM AF488 and IgG AF568 in dilutions 1:500 (Figure 11) and 1:1000 and Fab-specific goat-anti-mouse IgG FITC in dilutions 1:150, 1:200, and 1:300 (Figure 12). With IgG AF568, IgM488, and IgG FITC there was fluorescence detected in negative control from unspecific binding. When compared to 20 nM Fab2A4 + 1:500 AF488/AF568, no difference can be noticed. Most of the detected fluorescence was from unspecific binding and does not depend on the Fab2A4, because the results do not vary a lot from negative control (1:500 AF488 or AF568). The required exposure times were relatively long with IgM AF488 and IgG AF568. With IgG FITC the detected fluorescence is brighter with the combination of 20.8 nM Fab2A4 + 1:200 IgG FITC when compared to the negative control. With the combination of 20.8 nM Fab2A4 + 1:300 IgG FITC, the fluorescence level is similar to the negative control. IgG FITC is a Fab-specific antibody, but the intensity of FITC conjugate was lower when compared to more advantageous AlexaFluor dyes. FITC's ability to show differences in GTP concentrations based on its intensity is therefore limited when compared to AlexaFluor dyes. Based on these results, the IgM AF488 and IgG AF568 were not used further and IgG FITC was used for staining of the U87MG samples.

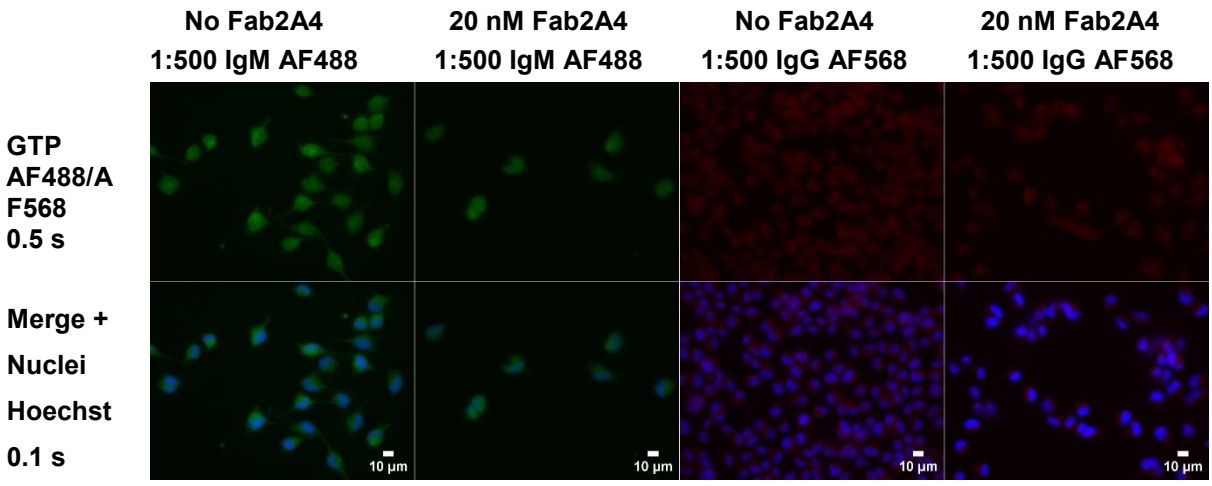

Figure 11. On the left negative control of IgM AF488 and on the second column the combination of 20 nM Fab2A4 + 1:500 IgM AF488. On the third column is the negative control of IgG AF568 as a secondary antibody and on the right the combination of 20.8 nM Fab2A4 + 1:500 IgG AF568. The HeLa cells were cultured for 24 h and then treated for 8 h. The scale bar is 10 µm and the exposure times were 0.357 s for AF488 and 0.1 s for Hoechst (nuclei).

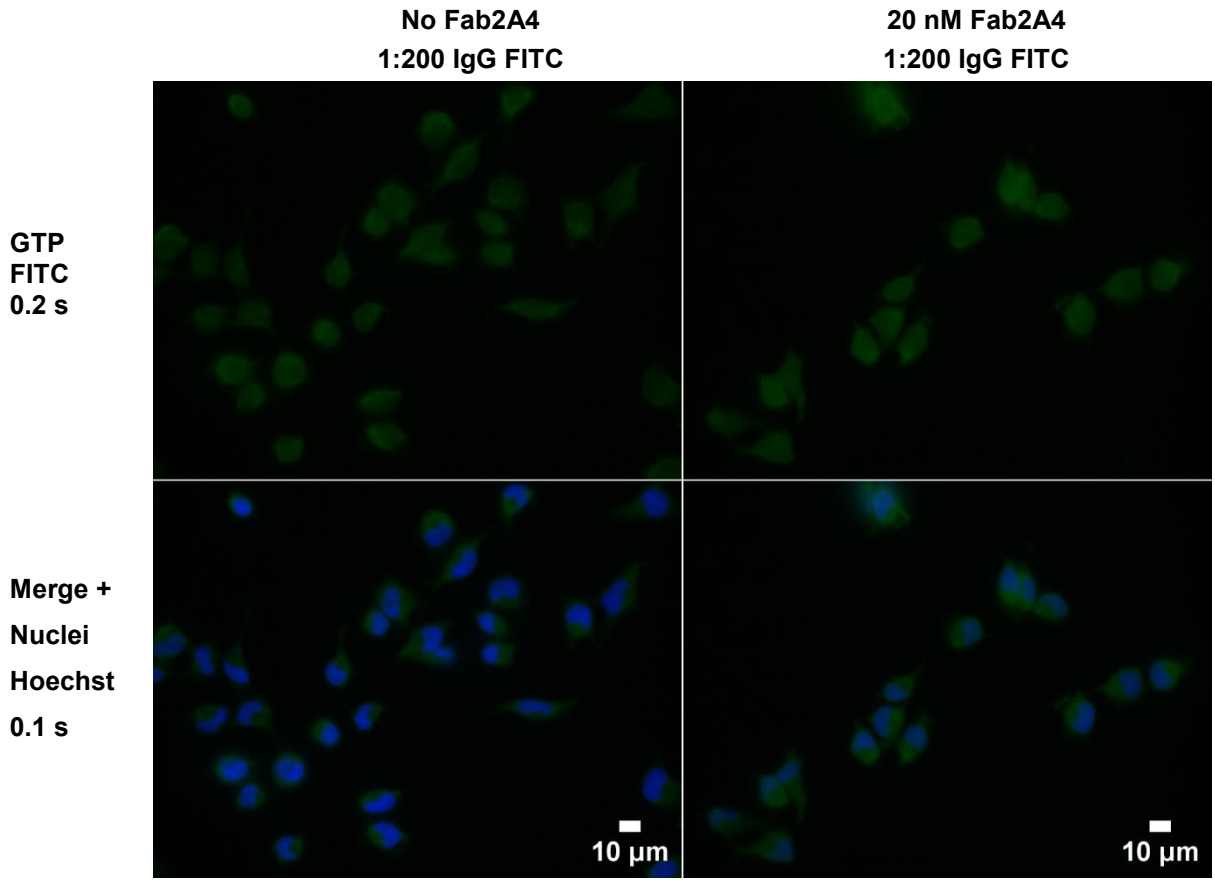

Figure 12. Fab-specific IgG FITC as a secondary antibody. On the left is the negative control without Fab2A4 and on the right is the combination of 20 nM Fab2A4 + 1:200 IgG FITC. The HeLa cells were cultured for 24 h and then treated for 8 h. The scale bar is 10 µm and the exposure times were 0.357 s for AF488 and 0.1 s for Hoechst (nuclei).

The antibodies for multicolour immunostaining with U87MG WT and DKO neurons were selected based on the results with HeLa cells. In multicolour immunostaining, the primary antibodies were 20 nM anti-GTP Fab2A4 or Fab2A4m and anti-IMPDH2 Ab (rabbit), and the respective secondary antibodies were Fab-specific goat-anti-mouse IgG FITC (1:400) or goat-anti-mouse IgG AF488 (1:1000) and goat-anti-rabbit IgG AF568 (1:400 or 1:1000). In the negative control without the primary antibodies, unspecific binding of the IgG FITC was detected, but the IgG AF568 was very selective and the fluorescence from unspecific binding was not detected (Figure 13). Also the background of the U87MG WT cells can be detected with the green wavelength (Figure 13).

The U87MG WT cells were cultured for 20 h and then treated for 6 h or 26 h or 33 h. In the 6 h treated cells (Figure 14), the RR effect of the IMPDH2-enzymes can be detected, but the effect is weaker when compared to the result after 26 h treatment (Figure 15). In guanosine-treated cells, the fluorescence from stained IMPDH2 enzymes was brighter when compared to the control (0.1% DMSO) and similarly to MPA samples, the effect was stronger after 26 h

treatment. In the cells which were treated for 6 h with 100 µM guanosine and 10 µM MPA, guanosine prevents indirectly the reversible aggregation of the IMPDH-enzymes. Aggregates were not detected and the fluorescence was diminished when compared to the guanosine-treated sample. The fluorescence level is closer to the control sample (DMSO). There was no significant difference between 26 h and 33 h treated U87MG WT cells. Based on these results, the 6 h and 26 h treatment time is long enough to cause the differences, but the effect was weaker with the 6 h treatment time and therefore it would be better to use longer treatment time. On the other hand, 33 h treatment was still suitable. With all the samples the fluorescence of Fab-specific IgG FITC and the negative control's unspecific binding were at the same level. Differences in GTP concentration between the treated samples could not be seen.

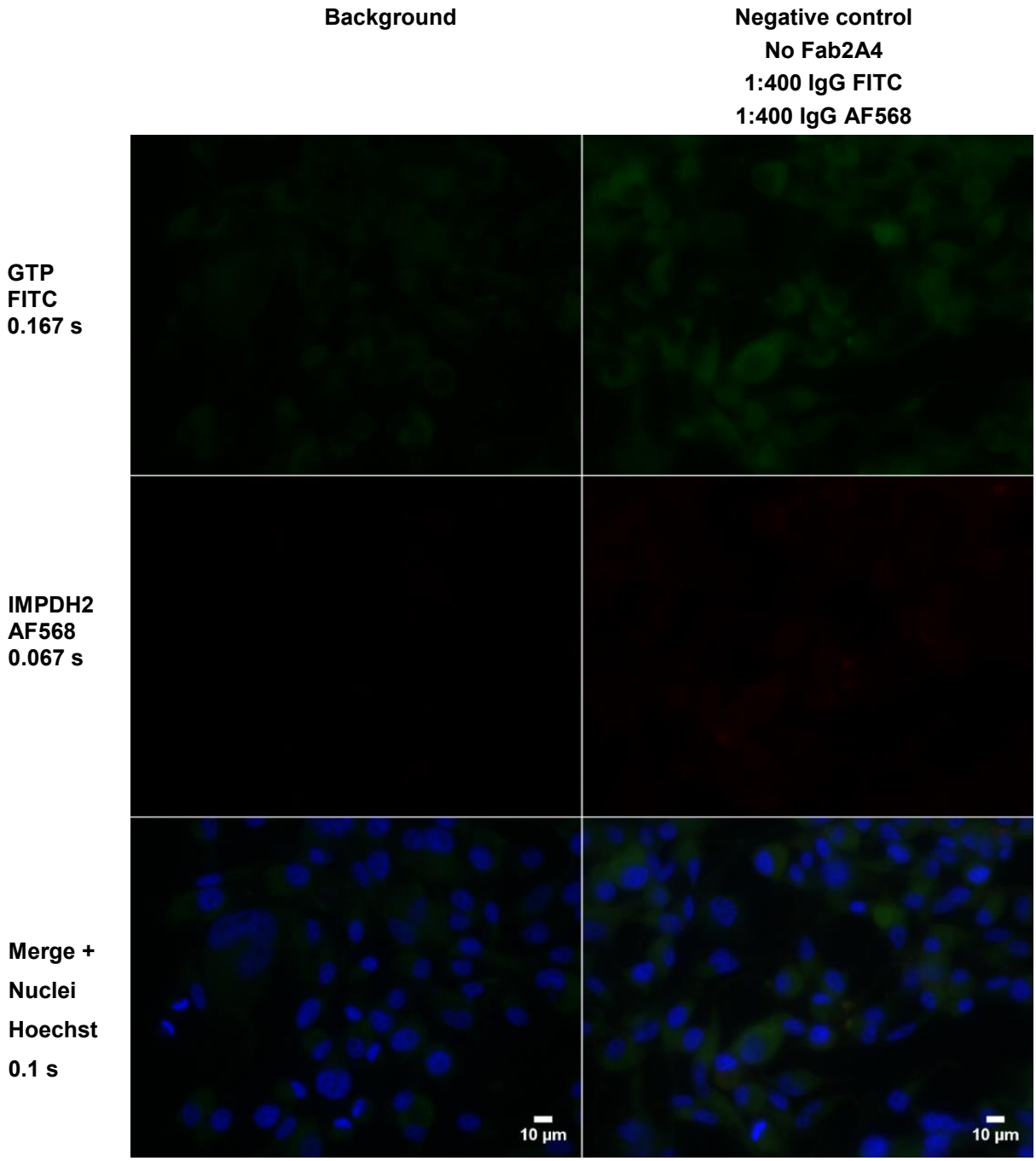

Figure 13. Negative controls of U87MG WT for multicolour immunostaining. The cells were cultured for 20 h and then treated for 26 h. On the left (without secondary antibodies) some background of the cells can be detected with the green wavelength. On the right is the negative control without primary antibodies (Fab2A4 and anti-IMPDH2). The secondary antibodies IgG FITC and IgG AF568 were used in dilution 1:400. The scale bar is 10 µm and the exposure times were 0.167 s for FITC, 0.067 s for AF568 and 0.1 s for Hoechst (nuclei).

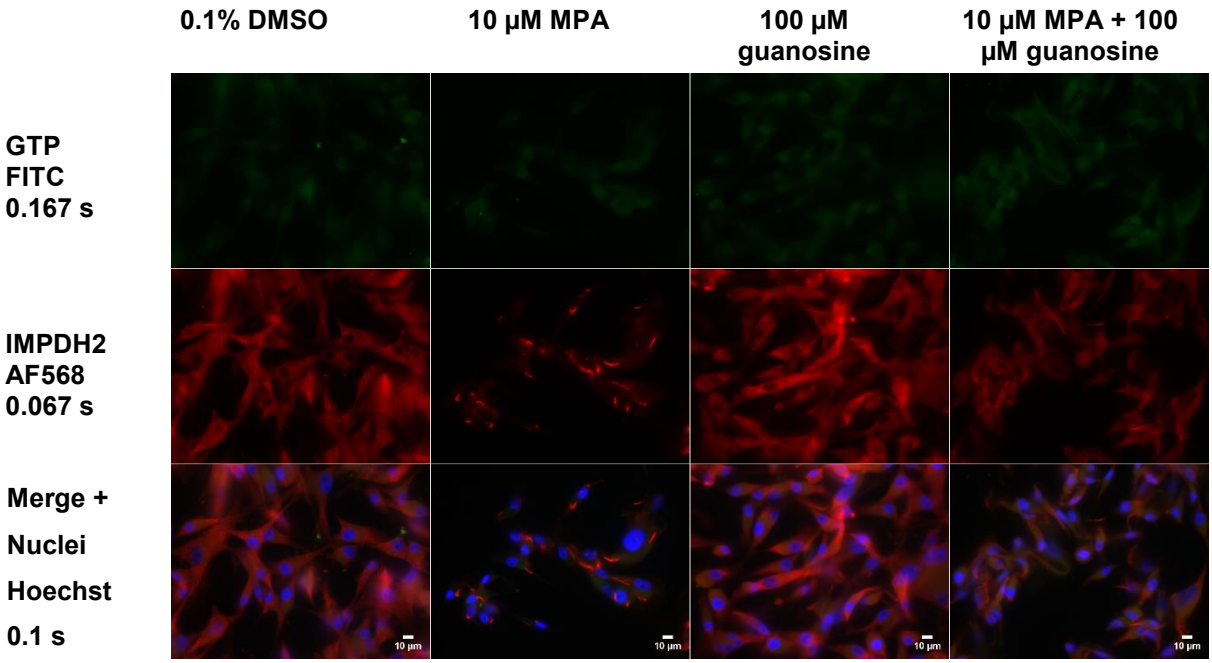

Figure 14. The multicolour immunostaining of the cultured (20 h) and treated (6 h) U87MG WT cells. The primary antibodies were 20 nM Fab2A4 and anti-IMPDH2 (rabbit, 1:400) and the respective secondary antibodies were IgG FITC (1:400) and IgG AF568 (1:400). The scale bar is 10 µm and the exposure times were 0.167 s for FITC, 0.067 s for AF568 and 0.1 s for Hoechst (nuclei).

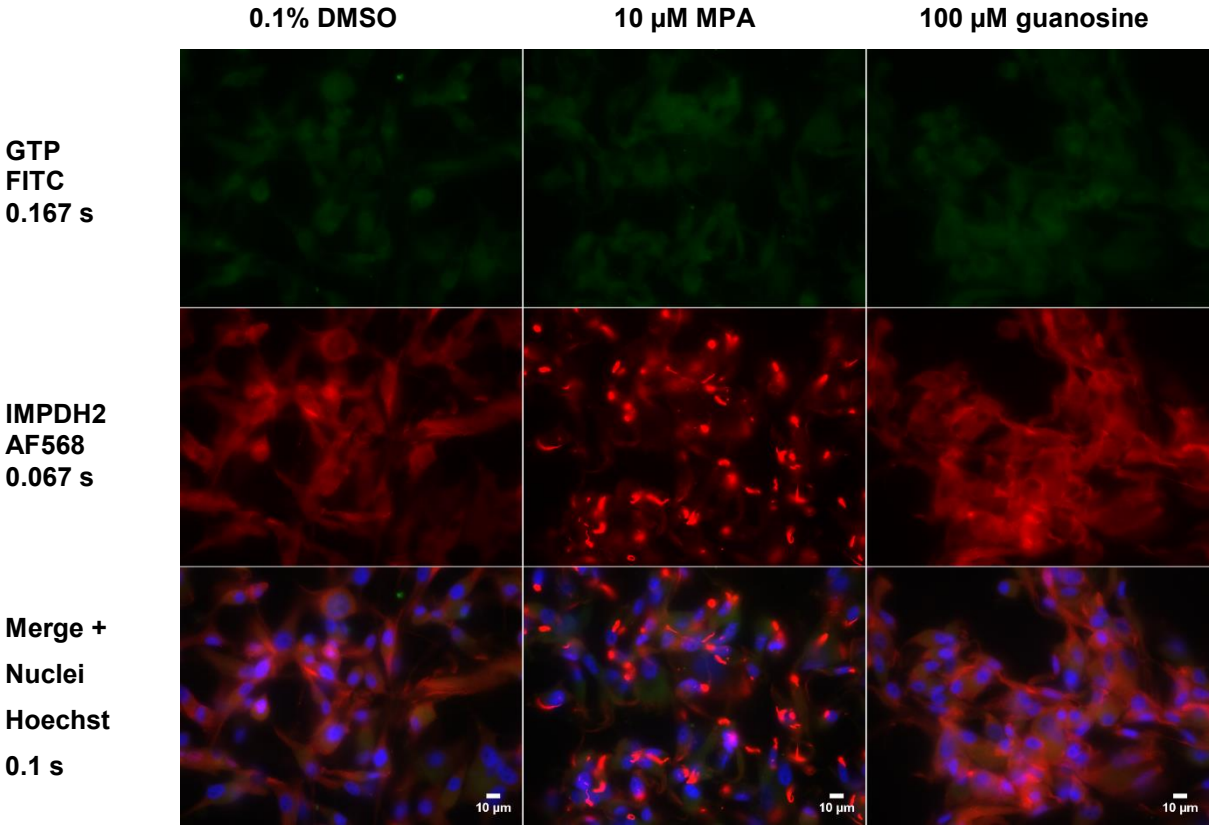

Figure 15. The multicolour immunostaining of the cultured (20 h) and treated (26 h) U87MG WT cells. The primary antibodies were 20 nM Fab2A4 and anti-IMPDH2 (rabbit, 1:400) and the respective secondary antibodies were IgG FITC (1:400) and IgG AF568 (1:400). The scale bar is 10 µm and the exposure times were 0.167 s for FITC, 0.067 s for AF568 and 0.1 s for Hoechst (nuclei).

With the multicolour immunostaining method, the U87MG IMPDH1/2-DKO cells were stained. The primary antibodies for DKO cells were 20 nM anti-GTP Fab2A4 and anti-IMPDH2 Ab (rabbit, 1:400), and the respective secondary antibodies were Fab-specific goat-anti-mouse IgG FITC (1:400) and goat-anti-rabbit IgG AF568 (1:400). 1xTBS-T was used in washes after the addition of primary antibodies. Instead of the chemical treatment, U87MG IMPDH1/2-DKO cells were co-cultured with U87MG WT or U87MG IMPDH1/2-DKO cells. The cells were co-cultured for 15 h or 26 h (Figure 16) or co-cultured for 48 h and then treated for 4 h with 10 µM MPA (Figure 17). The co-cultures were used to study the possible rescuing effect between the DKO and the WT cells. The aim was to show qualitatively with fluorescence microscopy whether the WT cells were rescuing DKO cells so that the GTP levels of the DKO cells would increase. In the co-culture system, cells on the bottom of the well and the cells on the membrane are separate but share the same medium and culturing conditions together. The pore size of the PET membrane inserts of the plate was either 8.0 µm or 1.0 µm, to study if the pore size causes any difference.

With all the samples the fluorescence of Fab-specific IgG FITC and the negative control's unspecific binding were at the same level. The exposure time used with DKO samples was the same as with the WT samples (0.167 s). This would indicate that most of the fluorescence is from unspecific binding and does not depend on the concentration of the GTP neither the Fab2A4. DKO/DKO cultures were used as a control sample and compared with DKO cells cultured with WT cells on the insert. Significant differences were not noticed. The results of imaging were similar with both pore sizes of the membrane (1.0 µm and 8.0 µm). Because the imaging of GTP with the selected secondary antibody IgG FITC did not show any differences in the GTP concentration, it could not be confirmed whether the pore size in the co-culture system causes any difference. There were DKO cells with more intensive signals from stained IMPDH2. The phenotype of those cells and areas seems to be closer to WT cells. Those cells were detected in both co-cultures (DKO/DKO and WT/DKO) and most likely it is not a rescuing effect caused by WT cells in the co-culture. Even though there was some fluorescence detected from the stained IMPHD2, the required exposure time for the imaging of IMPDH2 was six times longer than with the WT cells. This indicates that the levels of IMPDH2 are very low when compared to the WT cells. After the MPA treatment, the stained IMPDH2-enzymes in DKO cells were not aggregated similarly when compared to the aggregation of the enzymes in the WT cells. The treatment time (4 h) might be too short for DKO cells since the growth of DKO cells is much slower when compared to WT cells.

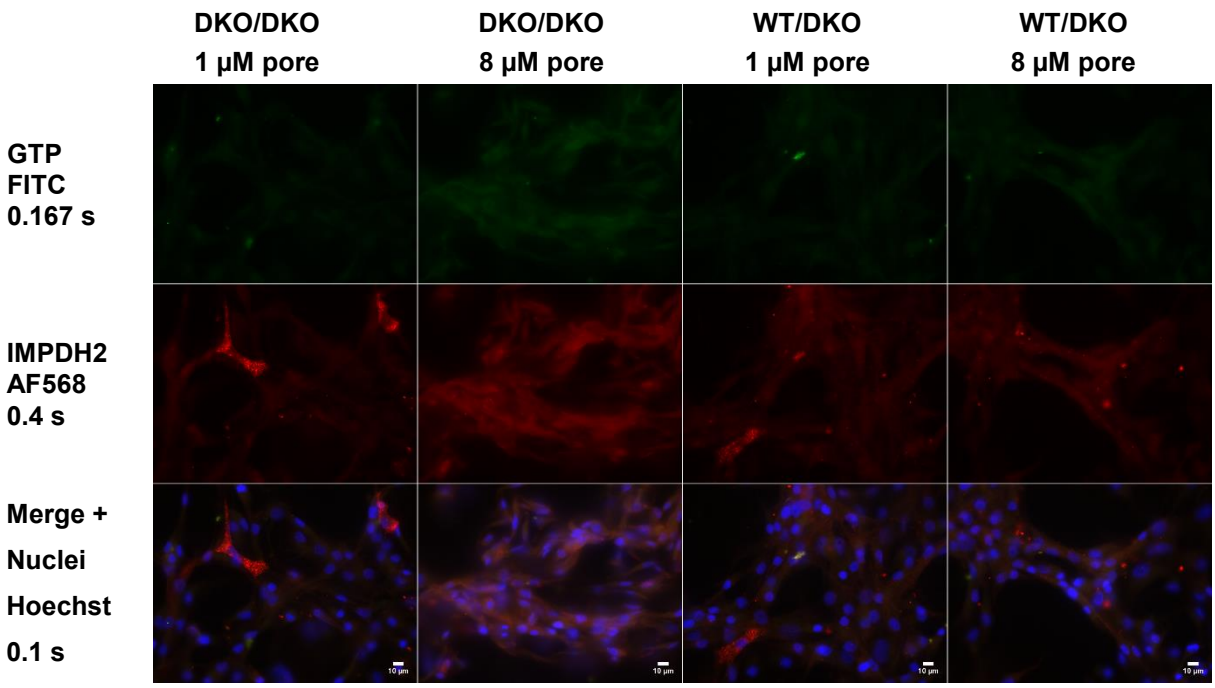

Figure 16. The multicolour immunostaining of the co-cultured (26 h) U87MG IMPDH1/2-DKO cells. The pore sizes 1.0 and 8.0 µm were used in the co-culture system. The primary antibodies were 20 nM Fab2A4 and anti-IMPDH2 (rabbit, 1:400) and the respective secondary antibodies were IgG FITC (1:400) and IgG AF568 (1:400). The scale bar is 10 µm and the exposure times were 0.167 s for FITC, 0.4 s for AF568 and 0.1 s for Hoechst (nuclei).

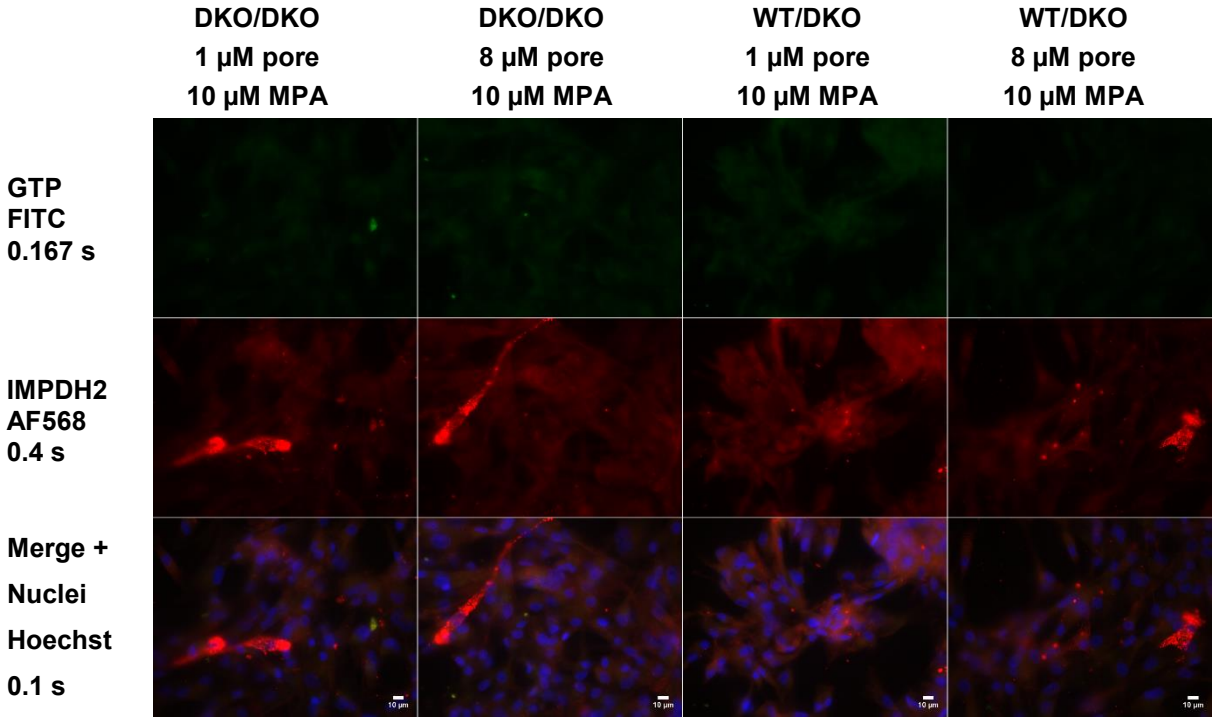

Figure 17. The multicolour immunostaining of the co-cultured (48 h) and MPA-treated (4 h) U87MG IMPDH1/2-DKO cells. The pore sizes 1.0 and 8.0 µm were used in the co-culture system. The primary antibodies were 20 nM Fab2A4 and anti-IMPDH2 (rabbit, 1:400) and the respective secondary antibodies were IgG FITC (1:400) and IgG AF568 (1:400). The scale bar is 10 µm and the exposure times were 0.167 s for FITC, 0.4 s for AF568 and 0.1 s for Hoechst (nuclei).

In multicolour immunostaining with the U87MG WT and DKO cells on the chamber glass slide the primary antibodies were 20 nM Fab2A4m and anti-IMPDH2 Ab (rabbit, 1:1000), and the respective secondary antibodies were goat-anti-mouse IgG AF488 (1:1000, new batch) and goat-anti-rabbit IgG AF568 (1:1000). The washing steps were done with PBS-T instead of TBS-T and the nuclei staining was done with DAPI in the Fluoromount-G at the mounting step instead of Hoechst. Also, the permeabilization and blocking steps were done differently. This time the permeabilization was done with 0.2% Triton X-100 instead of 0.5% saponin and the blocking step with 1% BSA instead of 10% goat serum. The cells were cultured for 15 h and the WT cells were then treated for 5 h. This combination of the antibodies was able to show differences in the GTP in addition to IMPDH2 after the treatments (Figure 18). Differences in the GTP level after the treatments were detected with the new stock of IgG AF488. In the MPA-treated WT cells, the fluorescence signal from IgG AF488 was also diminished. The rings and rods effect of the IMPDH2-enzymes can be detected after the MPA treatment. In guanosine-treated WT cells, the fluorescence from stained IMPDH2 enzymes and stained GTP was brighter when compared to the control (0.1% DMSO). In the WT cells which were treated with 100 µM guanosine and 10 µM MPA, the guanosine prevents indirectly the reversible aggregation of IMPDH-enzymes. Aggregates were not detected and the fluorescence from IMPDH2 and GTP was diminished when compared to the guanosine-treated sample and the results with both targets (GTP and IMPDH2) were in between the result of the additives alone (Figure 18).

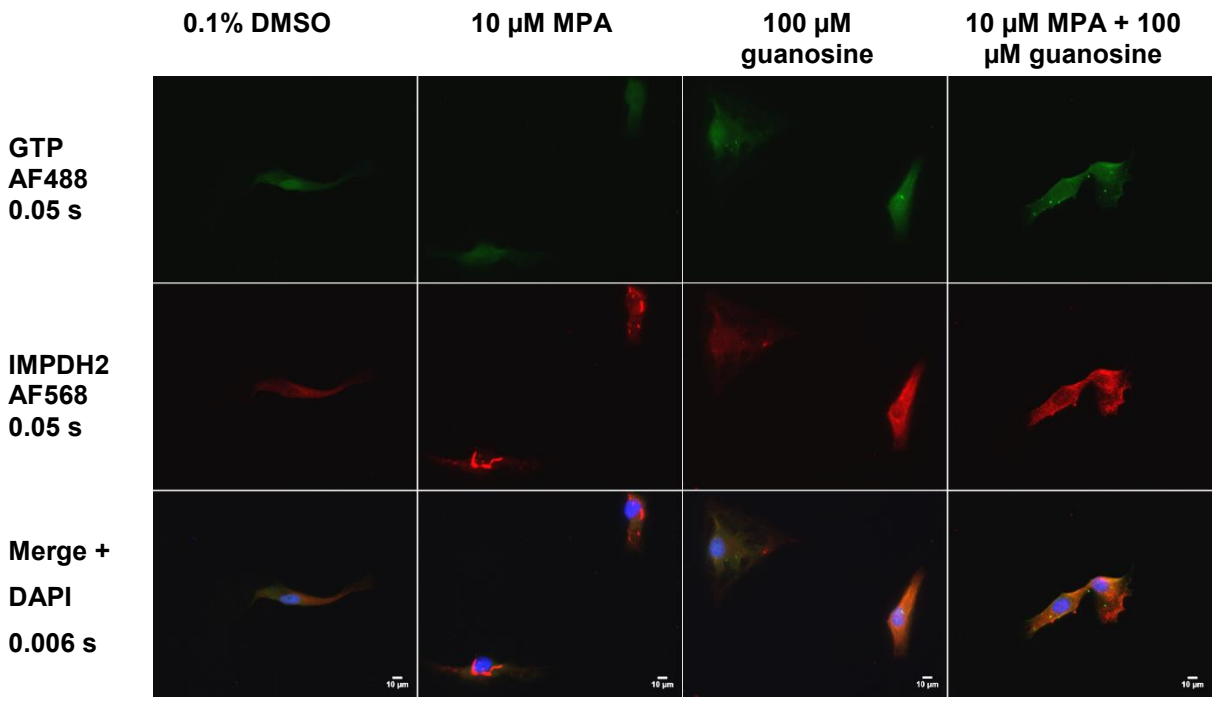

Figure 18. The multicolour immunostaining of the cultured (15 h) and treated (5 h) U87MG WT cells. The primary antibodies were 20 nM Fab2A4m and anti-IMPDH2 (rabbit, 1:1000) and the respective secondary antibodies were IgG AF488 (1:1000) and IgG AF568 (1:1000). The scale bar is 10 µm and the exposure times were 0.05 s for AF488 and AF568 and 0.006 s for DAPI (nuclei).

With the DKO cells, some fluorescence was detected from the stained IMPDH2 and GTP. Two exposure times were used for DKO cells, one more optimal for DKOs (longer exposure time) and then the shortest exposure time with which the targets can be seen (Figure 19). In comparison to the WT cells, the required exposure time for the imaging of GTP was almost three times and for IMPDH2 almost seven times longer than with the WT cells. Even with the longer exposure time, the fluorescence signal was significantly diminished when compared to clear signals from WT cells with shorter times (Figure 20). This indicates that the levels of GTP and IMPDH2 are low when compared to WT cells. Because the nucleolar size in U87MG DKO cells is decreased in comparison to U87MG WT[9], a longer exposure time of DKO cells was needed to get a similar signal (Figure 20).

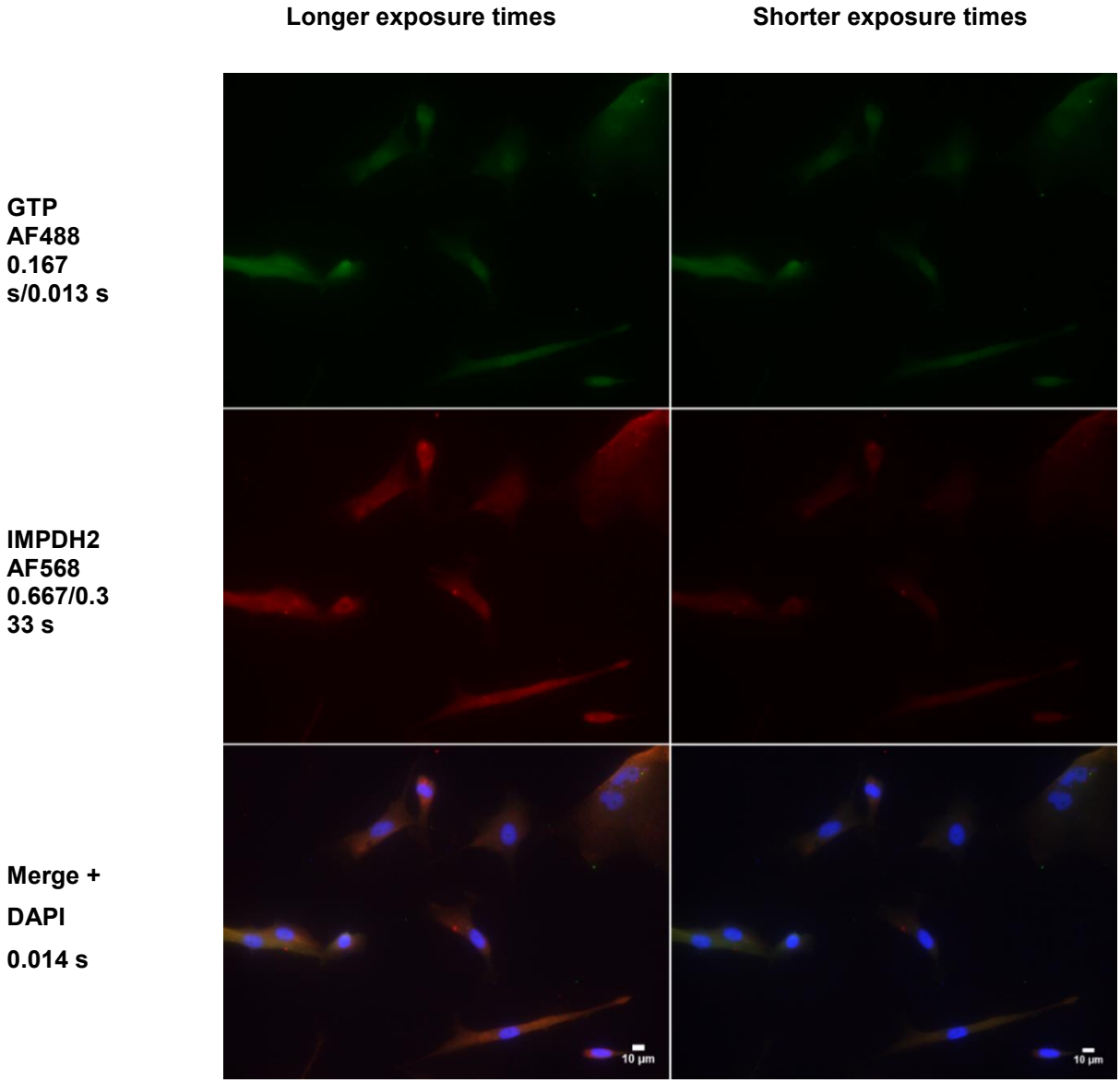

Figure 19. The multicolour immunostaining of the cultured (15 h) U87MG IMPDH1/2-DKO cells. The primary antibodies were 20 nM Fab2A4m and anti-IMPDH2 (rabbit, 1:1000) and the respective

secondary antibodies were IgG AF488 (1:1000) and IgG AF568 (1:1000). The scale bar is 10 µm and the exposure times were 0.167 s for AF488 and 0.667 s for AF568 on the left or 0.013 s for AF488 and 0.333 s for AF568 on the right and 0.014 s for DAPI (nuclei).

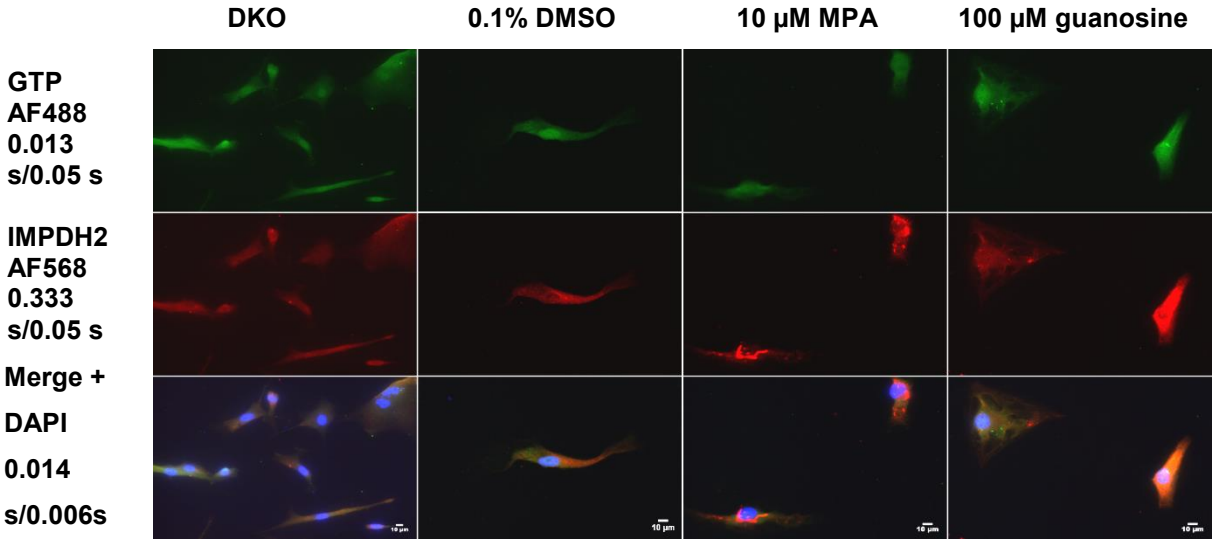

Figure 20. Comparison of the cultured (15 h) U87MG DKO cells and treated (5 h) WT cells. The primary antibodies were 20 nM Fab2A4m and anti-IMPDH2 (rabbit, 1:1000) and the respective secondary antibodies were IgG AF488 (1:1000) and IgG AF568 (1:1000). The scale bar is 10 µm and the exposure times were 0.013 s for AF488 and 0.333 s for AF568 and 0.014 s for DAPI (nuclei) in DKO cells (on the left) or 0.05 s for AF488 and AF568 and 0.006 s for DAPI (nuclei) in WT cells.

As a conclusion, the anti-GTP Fab fragment can be used for direct bioimaging of GTP. The optimisation steps were done with HeLa WT cells and the anti-GTP Fab2A4 and the final multicolour immunostaining for U87MG with the Fab2A4m. The Fab2A4m fragment seems to be more sensitive to show differences in the GTP concentration when compared to Fab2A4. This developed method with goat-anti-mouse IgG AF488 is able to show differences in GTP concentration. The functionality of GTP staining depends on the binding ability of the secondary antibody. The second stock of IgG AF488 with U87MG cells gave better results when compared to the first stock used with HeLa cells. Because the staining of the IMPDH2-enzyme was performed successfully every time, it can be expected that also the Fab fragment was able to bind to its cellular target and most likely there were no challenges for example with the permeabilization.

In the washing steps, the TBS-T was used most of the time instead of PBS-T after the addition of the antibodies to protect the Fab fragment from high salt concentrations and to reduce the background. Even though the Fab fragment is sensitive to high salt concentrations and may lose a part of its binding ability, the staining of the GTP does not depend crucially on the chemicals in the washing steps. With the most suitable secondary antibody IgG AF488 (the second stock), the washing steps were performed with 1xPBS-T but it did not increase the background distractingly or prevent the binding of the Fab fragment. Based on this, the

functionality of GTP staining depends on the binding ability of the secondary antibody and it can be expected that anti-GTP Fab binds to its target, but the faced challenges in imaging were caused by the inappropriate secondary antibodies and their poor binding ability to Fab fragment.

The direct imaging of cellular GTP and IMPDH2-enzyme was successfully performed with 20 nM Fab2A4m and anti-IMPDH2 Ab (1:1000, rabbit) as primary antibodies and the respective secondary antibodies were IgG AF488 (1:1000) and IgG AF568 (1:1000). With this developed multicolour immunostaining method, U87MG WT and IMPDH1/2-DKO cells were compared. In comparison to WT cells, the detected low signals from DKO cells required multiple times longer exposure times. This indicates that the levels of GTP and IMPDH2 are very low when compared to WT cells.

3.2 Proliferation assays with crystal violet

As a preliminary test for the co-culture, the U87MG WT and U87MG IMPDH1/2-DKO cells were used for proliferation assays observed with crystal violet. The aim of the assays with crystal violet was to observe the proliferation rate of the MPA-treated U87MG WT cells, which were rescued with the second rescue medium. The U87MG cells were first treated with 0.1% DMSO (control) or 10 µM MPA for 8 h and then the culture medium was changed. The second medium was the rescue medium: 0.1% DMSO (control), 50 or 100 µM guanosine medium or medium from the culture dish, which contained 50 µM or 100 µM guanosine at the beginning of the first treatment time (8 h). For one MPA-treated sample, the treatment medium was not changed to the rescue medium, to study the affect of longer MPA treatment on the proliferation of the cells. The measured absorbance of crystal violet is proportional to the proliferation of the cells.

The absorbance was at a similar level with all the samples after 12 h to 24 h culture with the rescue medium. Differences in the proliferation appeared after a longer rescue time from 43 h to 92 h. When comparing different guanosine rescue mediums (Figure 21), the lowest absorbance and proliferation were detected with the MPA-treated cells with the rescue mediums of 100 µM guanosine and 50 µM guanosine from another culture. This can be explained by the possible toxic effect of too high guanosine concentration (100 µM). When it comes to 50 µM guanosine from another culture, it is possible that there were not enough nutrients and guanosine left to rescue the MPA-treated cells. The absorbance of the control samples (not treated with MPA) was in the middle. The highest absorbance was measured

from MPA-treated samples rescued with 50 µM guanosine and 100 µM guanosine from another culture. Based on this 50 µM guanosine medium is optimal for the proliferation of the cells. Most likely, 100 µM guanosine medium from the other culture has the optimal level of guanosine (closer to 50 µM than 100 µM), because the first culture has already consumed part of the guanosine. Based on these results, 50 µM guanosine medium was selected for use in further proliferation studies with crystal violet and GTP-ATP assay.

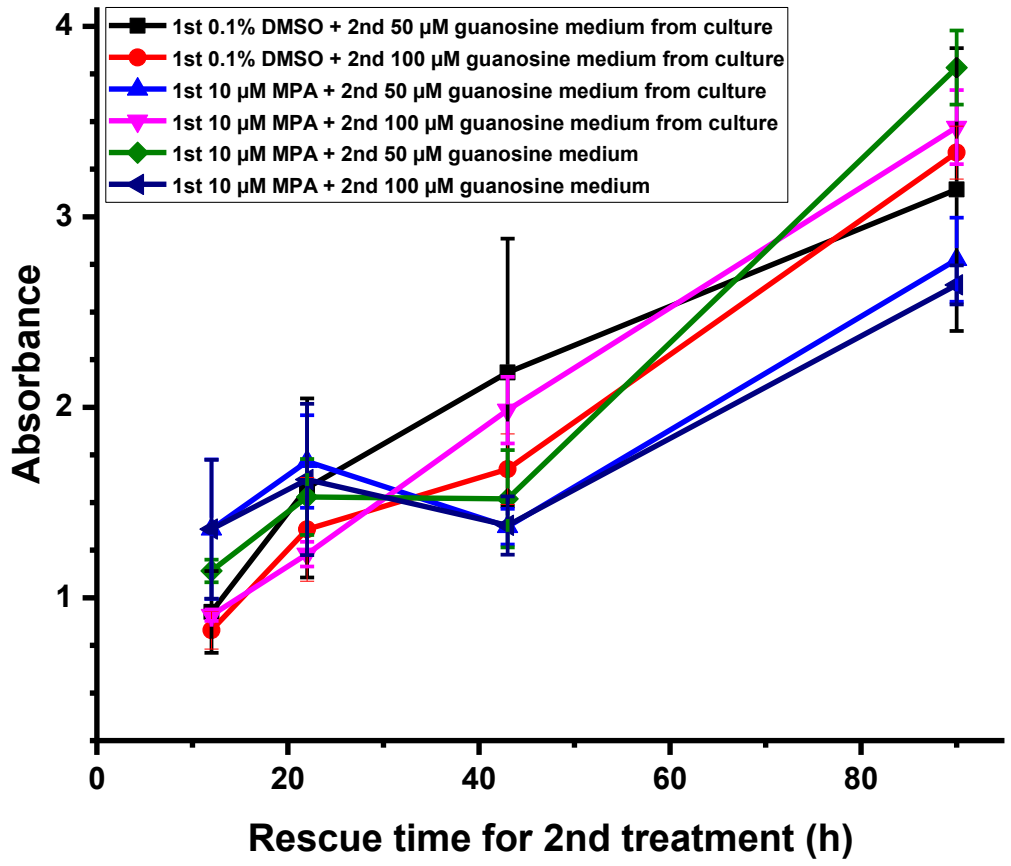

Figure 21. The comparison of the proliferation (proportional to absorbance) of the U87MG WT cells after different rescue mediums containing guanosine.

Different rescue mediums were compared between DMSO-treated and MPA-treated cells (Figure 22). The black line describes the proliferation of the untreated cells: first the proliferation stays at the highest, but between 42 and 90 hours almost all the samples were proliferating faster. At the 90 h time point, the sample treated with DMSO and having DMSO-medium as a rescue medium was on the same level as the untreated sample, as expected. The highest absorbance was measured from the sample which was treated with DMSO and then had fresh medium as a rescue medium, and the MPA-treated sample which has 50 µM guanosine medium as a rescue medium. Based on this, guanosine has the ability to rescue the MPA-treated cells to the normal level (DMSO-treated control samples). The MPA-

treated samples rescued with 50 µM guanosine from another culture (dark blue line) or DMSO medium from another culture (green line) were in the middle with the DMSO-treated sample which has 50 µM guanosine medium from another culture (pink line). Based on this, the rescue medium is working even without the additional guanosine. This would indicate that there are other rescue mechanisms as well and the medium from another culture has the ability to rescue MPA-treated cells without the additional guanosine. Most likely the lack of nutrients was reducing the proliferation with all these samples when compared to the samples with the highest absorbance, which both were having fresh medium (not from another culture).

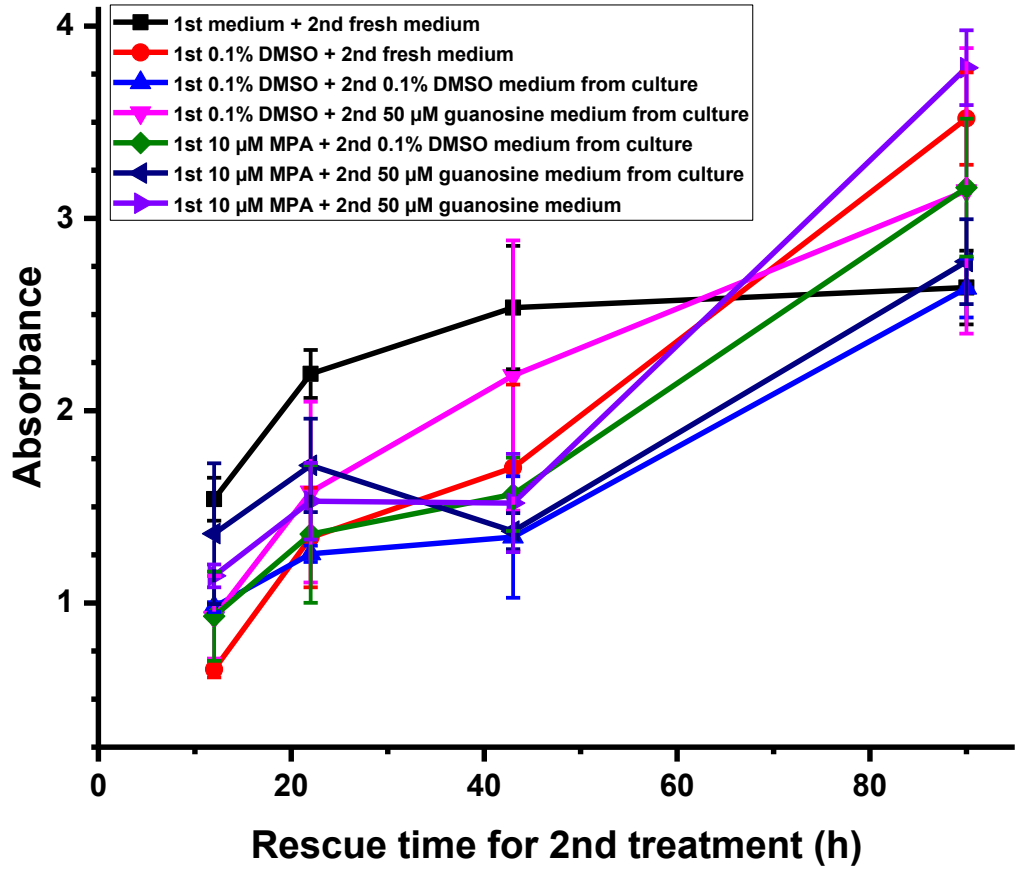

Figure 22. The comparison of the proliferation (proportional to absorbance) of the DMSO-treated (control) and MPA-treated U87MG WT cells after different rescue mediums.

MPA inhibits indirectly the proliferation of the U87MG WT cells (Figure 23A) and DKO cells (Figure 23B) and the measured absorbance stays low under constant MPA treatment when compared to other samples. On the other hand, the lack of nutrients was also limiting the proliferation since the medium was not changed. With DKO cells this could be the dominant reason since DKO cells do not express the IMPDH enzymes which MPA is inhibiting. As expected, the second lowest absorbance was measured from the MPA-treated

samples with 0.1% DMSO medium as a rescue medium. The inhibiting effect is then removed and the cells were able to recover and proliferate faster. The control sample was first treated with 0.1% DMSO and after 8 h treatment time, the new 0.1% DMSO medium was changed. The measured absorbance of the control sample was in the middle when compared to other samples. The fastest proliferation and the highest absorbance were measured from the DMSO-treated and MPA-treated samples, which had the rescue medium from another WT culture. With the WT cells, the highest absorbance was measured from the DMSO-treated sample, but the absorbance of the MPA-treated sample was almost at the same level. With DKO cells the order was reversed to WT cells and both samples had similar absorbance. Because DKO cells do not express the IMPDH enzymes which MPA is inhibiting, the recovery from MPA treatment could be faster and the result is similar to the DMSO-treated cells. With WT cells, the absorbance after the guanosine rescue medium from another WT culture was significantly higher when compared to the control sample. This indicates the important role of guanosine in rescuing effect after MPA treatment.

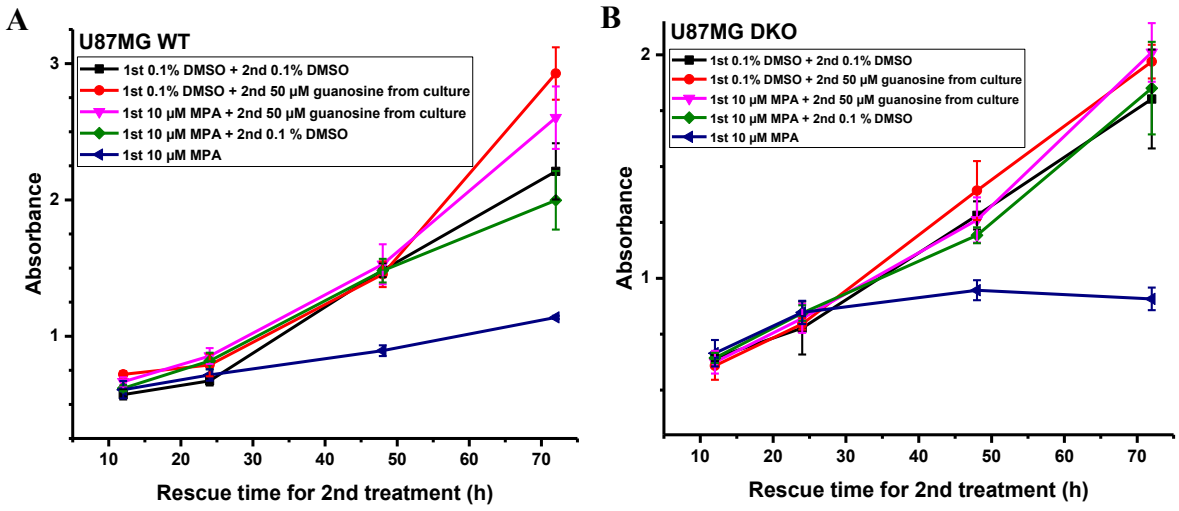

Figure 23. The comparison of the proliferation of the DMSO-treated (control) and MPA-treated U87MG WT cells (A) and DKO cells (B) after different rescue mediums.

The comparison of the U87MG WT and the DKO cells (Figure 24A) shows the differences between the cell strains under the rescue treatments. The lowest absorbance was measured from WT cells under a constant MPA medium. On the other hand, the lack of nutrients was also limiting the proliferation since the medium was not changed. The proliferation of the DKO cells was similar to the MPA-treated WT sample with DMSO-medium as a rescue medium. It was important to notice that the MPA-treated cells were actually proliferating slower than DKO cells. If the proliferation of the DKO cells is imitated, first MPA-treated and then DMSO-treated cells have a similar proliferation rate.

The rescue mediums of the DKO samples were DMSO-medium or medium from another WT culture containing guanosine. The significantly highest absorbance was measured from the MPA-treated WT sample which had the rescue medium from another WT culture (containing DMSO). The recovery effect of the WT cells was significant when compared to the guanosine-treated DKO cells, which were proliferating slower despite the additional guanosine. This indicates the rescuing effect of the medium from another WT culture is significant for WT cells even without the added guanosine. The medium was rescuing the MPA-treated cells in other mechanisms as well.

The comparison of the WT and the DKO cells (Figure 24B) shows the differences between the cell strains under the same rescue treatments. In this comparison, the absorbance measured from DKO cells was similar to the MPA-treated WT sample with DMSO-medium as a rescue medium. The rescue mediums of the DKO samples were DMSO-medium or medium from another WT culture containing guanosine. Based on these results the MPA treatment was not affecting much to DKO cells and the measured absorbance is at a similar level between MPA-treated and DMSO-treated DKO cells. The significantly highest absorbances were measured from the WT samples which had the guanosine-containing rescue medium from another WT culture. This indicates the rescuing effect of the medium from other WT culture is significant and the added guanosine can also boost the recovery of the WT cells after MPA treatment.

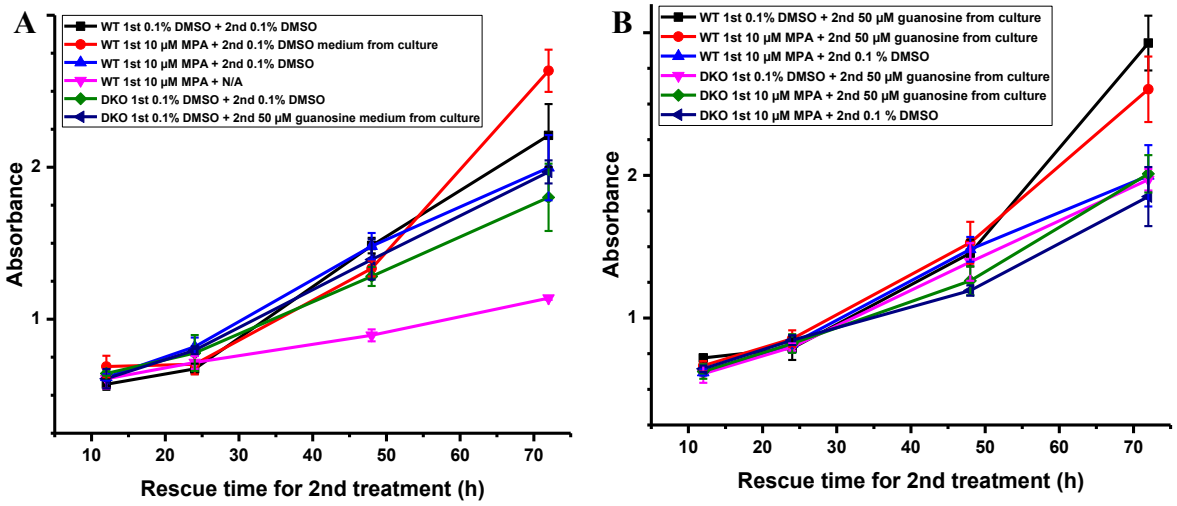

Figure 24. The summarising comparison of the absorbance of the U87MG WT and DKO cells after rescue treatments.

Based on these results the rescue effect to MPA-treated WT cells is significant with the rescue medium from another WT culture. For the guanosine addition, a concentration of 50 µM was a safer option for the cells since 100 µM guanosine seems also to have some toxic effects

which can be noticed as decreased absorbance and proliferation of the cells. Guanosine can boost the rescue, but the effect is stronger with WT cells. The rescue medium containing DMSO can help the recovery of WT cells if the medium is not too old and there are enough nutrients. The rescue effect appeared after a longer culturing time, 43 h to 92 h. The rescue effect was not significant with DKO cells but the DKO cells are proliferating slower when compared to WT cells. It is possible that the rescue time was too short for DKO cells and the differences would have appeared after a longer time of rescue.

3.3 GTP-ATP assay

The 2'-/3'-AHC-GTP was conjugated with Eu^{3+}-chelates for the detection solution of the GTP-ATP assay and purified with HPLC (Figure 25). The retention time of the 9-dentate Eu^{3+}-chelate (4-[2-(4-isothiocyanatophenyl)ethynyl]-2,6,-bis{[N,Nbis(carboxymethyl)-amino]methyl}pyridine europium(III), bearing one additional iminodiacetate coordinating arm) alone was 22 min (black line). The labelled GTP eluted in three main peaks in 12-16 min (red line) and the GTP alone at 5-7 min. All the peaks were collected. The actually used Eu^{3+}-chelate-GTP had {2,2',2",2'"-{[4'-(4'"-isothiocyanantophenyl)-2,2',6',2"-terpyridine-6,6"-diyl]bis(methyleneinitrilo)}tetrakis(acetato)}europium(III) Eu^{3+}-chelate, and it was purified similarly earlier.

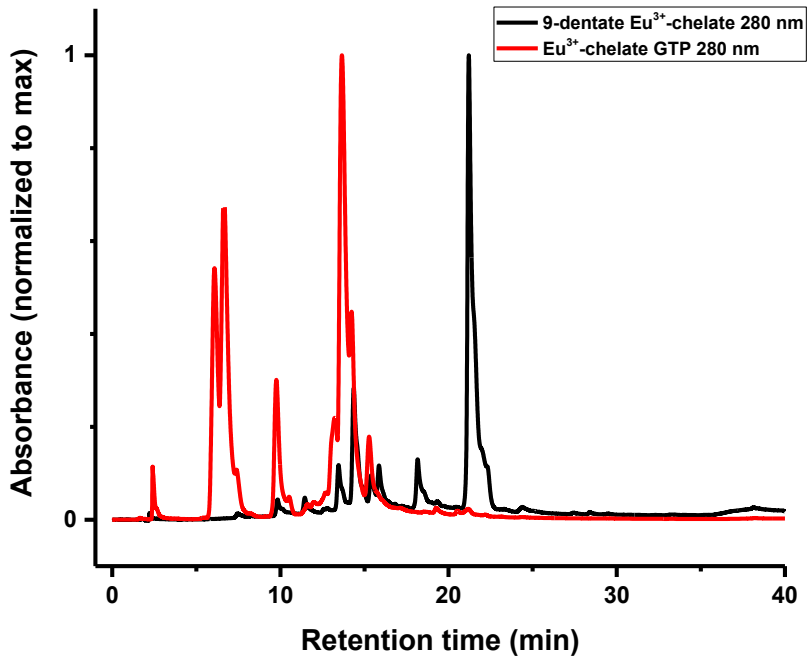

Figure 25. The representative chromatograms of the purification of the Eu^{3+}-chelates and conjugated GTP with HPLC. Each chromatogram was normalized to its maximum absorbance.

The anti-GTP Fab2A4 and the Eu^{3+}-chelate conjugated GTP were utilized in a high throughput 384 format to quantify the GTP concentration in solution from the cell-based (U87MG) samples. In the workflow (Figure 26), cultured and treated cells were collected and the nucleotides were precipitated with 80% MeOH (16 000g centrifugation for 10 min). The GTP assay was performed from the diluted cell lysate. The final concentration of nucleotides of the sample in the assay buffer should be on a nanomolar scale (10–1000 nM). The GTP of the sample and the produced Eu^{3+}-chelate labelled GTP competes in binding to Fab2A4 and a soluble quencher molecule MT2 is quenching the TRL-signal of the free Eu^{3+}-chelate-GTP (ex. 340 nm, em. 620 nm, integration and delay times 400–800 μs) in the solution (Figure 27). The modulator can not reach the complex of Fab2A4 and bound Eu^{3+}-GTP and therefore the energy transfer between the Eu^{3+}-chelate and modulator does not occur and the TRL emission of Eu^{3+}-chelate-GTP can be measured at the wavelength 620 nm. When the binding site of Fab is filled by the sample's GTP, the distance between soluble modulator molecules and free Eu^{3+}-chelate-GTP in the detection solution decreases and energy transfer increases, which leads to quenching of the signal. Based on the detected emission signal, the concentration or the amount of substance of GTP can be determined from the linear range of the standard curve. When the GTP assay was combined with a commercial ATP kit, the ATP-GTP ratios were able to be studied, giving more information about the energetic state of the cells. The ATP kit (AAT Bioquest) utilizes luciferase enzyme which catalyses an oxidation of luciferin to detect ATP in the homogenous assay form. First, the ATP is required for activation of the protein to produce an anhydride intermediate which then reacts with oxygen to a transient dioxetane. The dioxetane breaks down fast to oxyluciferin and carbon dioxide and emits light at 560 nm. This luminescence can be detected with a chemiluminometric microplate reader, and it is proportional to the concentration of ATP when ATP is the limiting reagent. The half-life of the luminescence signal is 2 h and the limit of detection is 50 cells per well.[31]

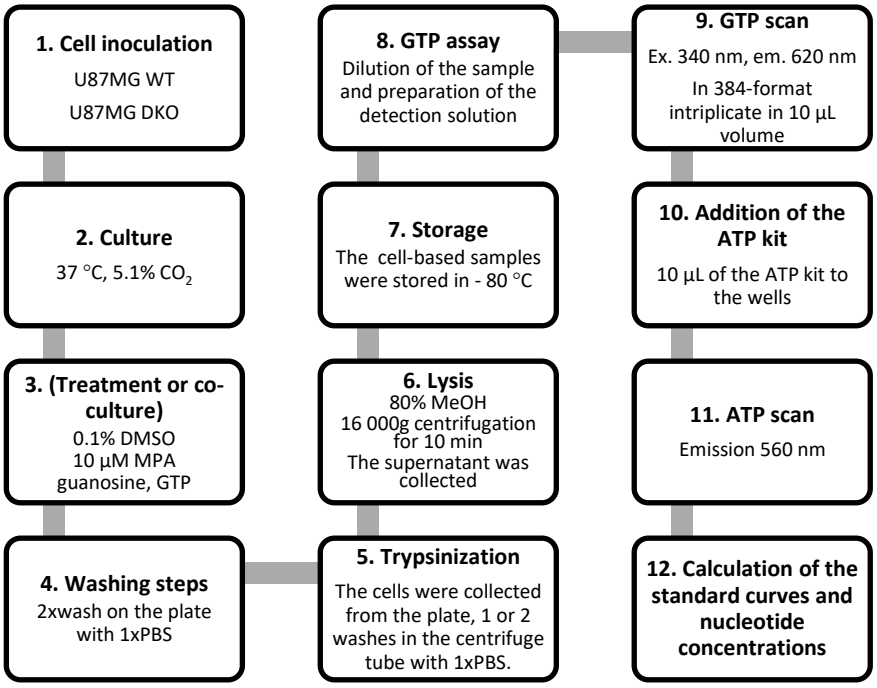

Figure 26. The workflow of the GTP-ATP assay.

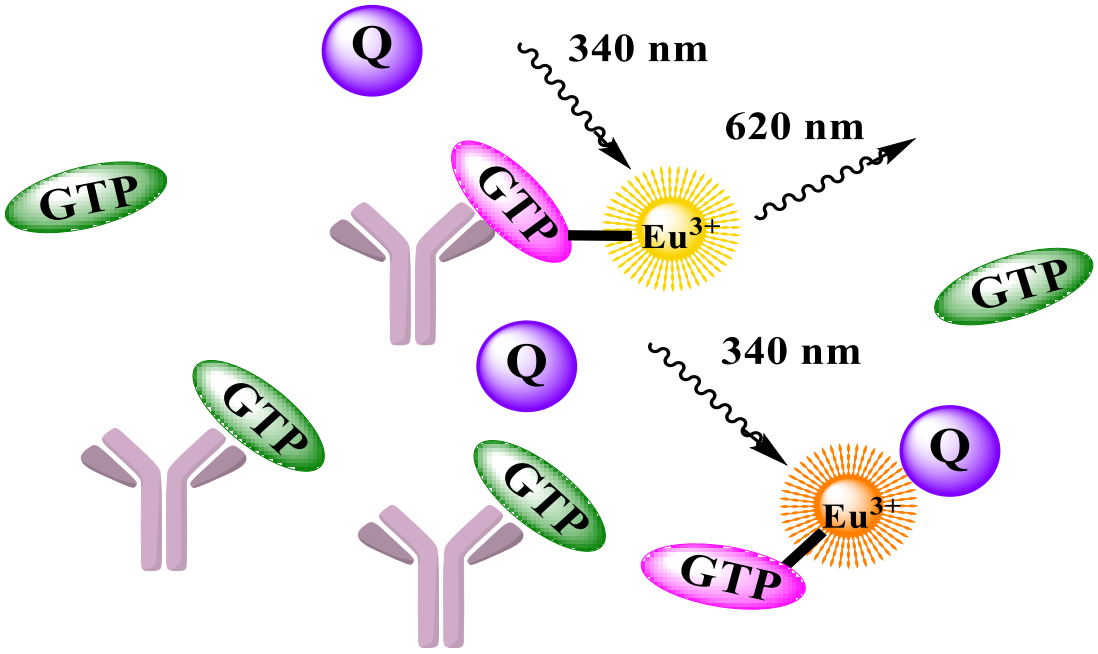

Figure 27. The detection of GTP. The GTP of the sample (green) and the produced Eu^{3+}-chelate labelled GTP (pink) competes in binding to Fab2A4 and a soluble quencher molecule MT2 (purple) is quenching the TRL-signal of the free Eu^{3+}-chelate-GTP (ex. 340 nm, em. 620 nm) in the solution.

GTP and ATP assays were performed in a sequential manner from the same well and concentrations were determined against the known standard solutions. The linear range of both assays was from 10 to 1000 nM and the standard curve (Figure 28) has TRL or luminescence signal as a function of the amount of substance in fmol (10^{-15}) in a logarithmic scale ($\log_{10}$). In a linear range of the GTP assay, the signal-to-background (S/B) ratio obtained

was 5, and the coefficient of variation (CV%) was below 5%. In a linear range of the ATP assay, the signal-to-background (S/B) ratio obtained was 100, and the coefficient of variation (CV%) was below 5%. Based on the cell titration curve of the GTP assay, the suitable amount of U87MG cells in the well varies between 800 to 8 000 cells (Figure 29A). With the ATP assay, the range of suitable amount of cells was a bit lower, from 200 to 8 000 cells (Figure 29B). Based on these results the target in cell number was approximately 1 000 to 2 000 cells per well with WT samples. With DKO samples the target in cell number was approximately 5 000 to 10 000 cells per well, because of the lower level of nucleotides (especially GTP) in DKO cells.

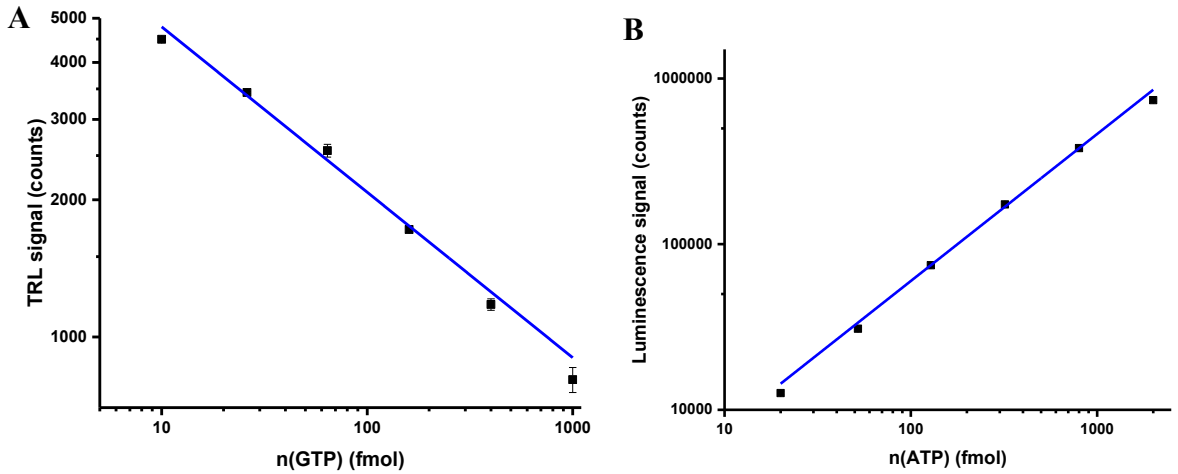

Figure 28. The standard curves of the GTP (A) and ATP (B) assay. The measured signal is as a function of the amount of substance. The linear range of the GTP assay was from 10 to 1 000 fmol in 10 µL final volume (A) and the linear range of the ATP assay was from 20 to 2 000 fmol in 20 µL final volume (B). The linear range of both assays was therefore from 10 to 1 000 nM.

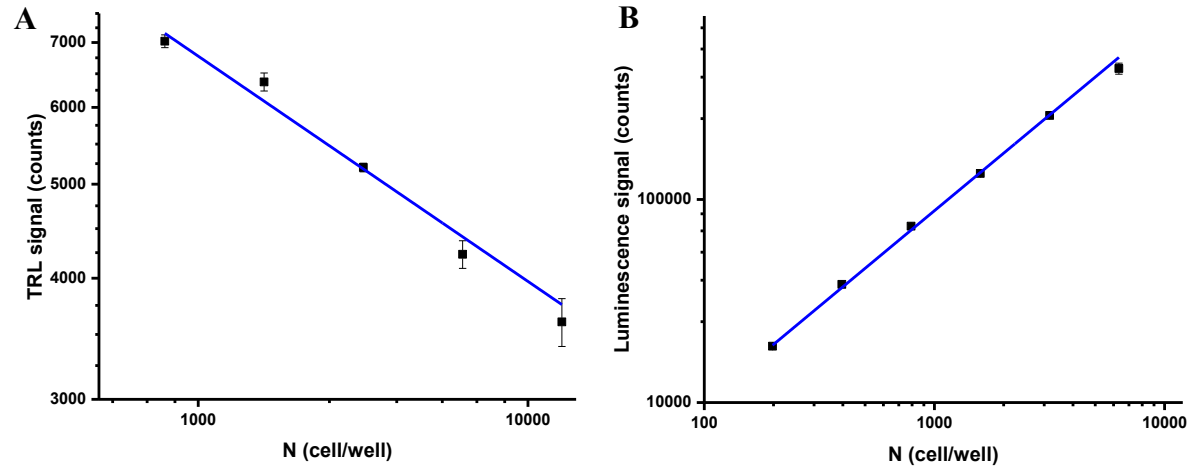

Figure 29. The cell titration curve of the GTP assay (A) and ATP assay (B) with U87MG WT cells. The measured signal is as a function of the cell number per well.

The ATP-GTP ratio is a simple tool to follow the effect of the treatments. Because the cell number used varied between the samples, the ratio is a more stable parameter to use when comparing to exact concentrations. Also, the ratio does not change despite the possible cell loss during the preparation steps. The cell volume used in the calculations for concentrations is also a possible source of error since the cell volumes vary between different cell lines and strains. The cellular ATP-GTP ratio after MPA treatment was followed from 2–120 h (Figure 30). At the 2 h timepoint, the ATP-GTP ratio of the cell-based samples is at the same level as the untreated sample (0 h). The first significant change in ATP/GTP ratio was monitored after 4 h treatment time and no further changes occurs in later time points. The ATP-GTP ratio increases when the cellular GTP concentration decreases because of the MPA's inhibiting effect on the GTP-synthetic IMPDH enzymes. The ATP-GTP ratio decreases slowly after 1 day of treatment time and stays at a constant level for days. Based on these results, from 4 h to 6 h treatment time is long enough to cause a significant change in ATP-GTP ratio for U87MG WT cells. After one day of treatment time, the ATP-GTP ratio slightly decreases and then stays constant for days.

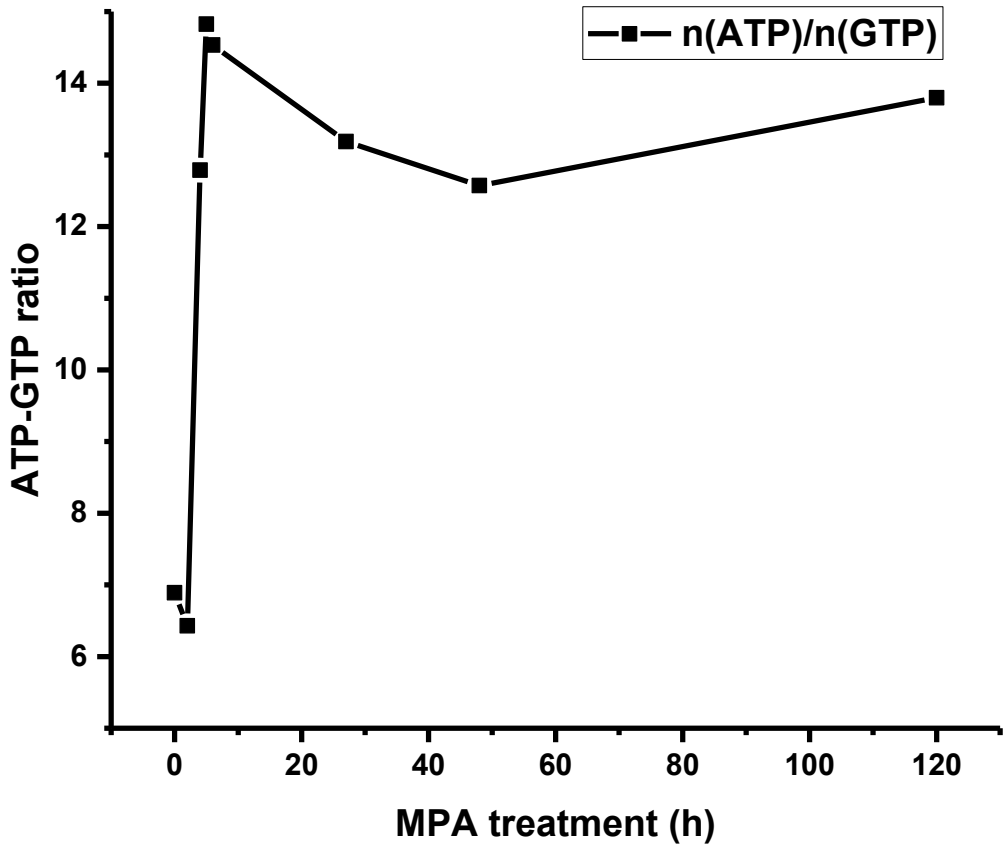

Figure 30. The timeline of the MPA treatment.

The ATP-GTP ratio is a simple tool to follow the effect of the treatments. The exactly calculated nucleotide concentrations per cell could have more error because of the long sample preparation and the possible cell loss during it. The U87MG WT cells were cultured for 24 h and then treated with 10 µM MPA, 50 µM or 100 µM guanosine medium for 10–24 h (Figure 31). Because all the additives were in DMSO, the control for the treatments was 0.1% DMSO. This control sample was also compared with the untreated sample. The ATP-GTP ratio between untreated and control samples is at the same level (ratio 7–8), which means DMSO alone is not affecting the ratio significantly. When compared to the untreated sample, MPA treatment significantly increases the ATP-GTP ratio: the GTP concentration decreases and the ATP concentration seems also to increase. 50 µM guanosine increases the concentration of GTP, which slightly decreases the ATP-GTP ratio when compared to the control sample. After 100 µM guanosine treatment, the ATP-GTP ratio increases and the GTP concentration decreases when compared to the control sample. This effect can be explained by the toxic effect of too high guanosine concentration. Based on this, the 50 µM guanosine treatment would be better and have a more beneficial effect on the cellular ATP-GTP ratio.

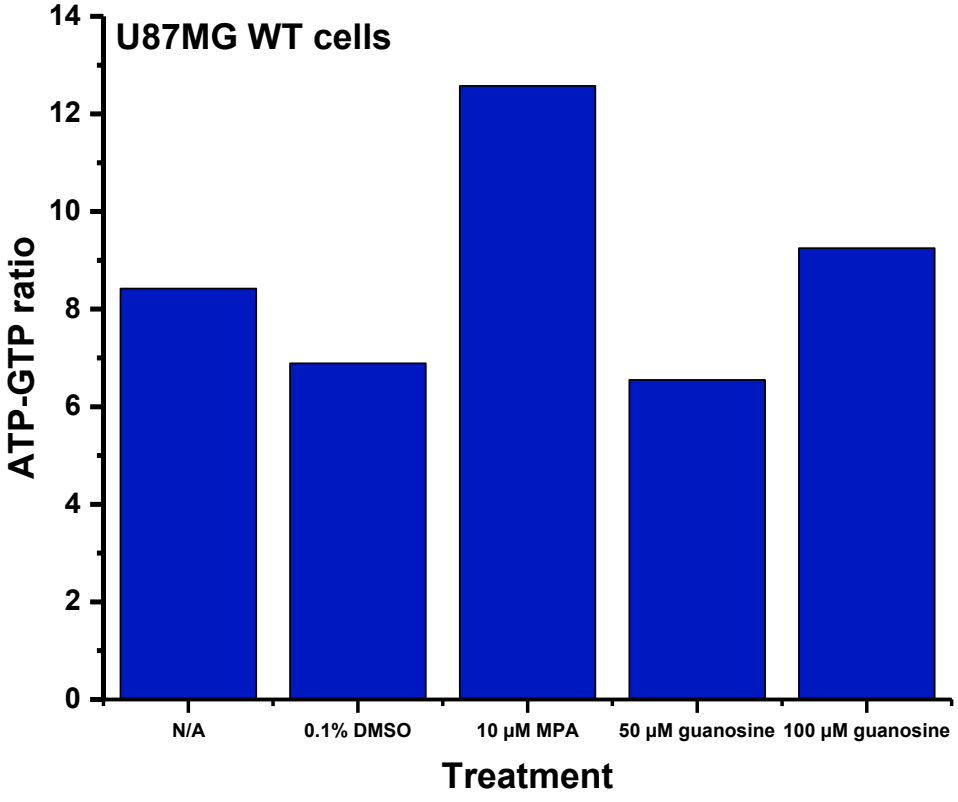

Figure 31. The results of the cell-based U87MG WT samples. When compared to the normal level, MPA treatment increases the ATP-GTP ratio. 50 µM guanosine slightly decreases the ATP-GTP ratio by increasing the cellular GTP. 100 µM guanosine treatment increases the ATP-GTP ratio because of the toxic effect of high guanosine concentration.

The U87MG DKO cells were cultured for 48 h or 150 h to measure the normal nucleotide levels of DKO cells and to detect if it is changing during the long culture time (Figure 32). These long culture times were used because the proliferation rate of the U87MG DKO cells is slower when compared to the WT cells. The GTP concentration in the cells did not change significantly, but the ATP-GTP ratio increases to 17 because of the increased ATP. The DKO cells were treated with 50 µM GTP and 50 µM guanosine for 48 h. As expected, the GTP concentration increased and the ATP-GTP ratio decreased significantly after both treatments when compared to the untreated DKO cells. With 50 µM guanosine, the ATP-GTP ratio decreased to 2.5 and the GTP concentration increased more when compared to GTP-treated cells because guanosine is the precursor of GTP and can be used easily in the production pathways of GTP in the cells. Added GTP is a larger molecule and is negatively charged due to the phosphate groups and its transportation into the cells requires active transportation through the cell's plasma membrane. The addition of GTP increases the intracellular GTP concentration and decreases the ATP-GTP ratio significantly from 10 to 5 when compared to the untreated sample. It can be expected that all the GTP of the medium was washed from the samples with many washing steps and it was not affecting the results. All the measured GTP was therefore intracellular.

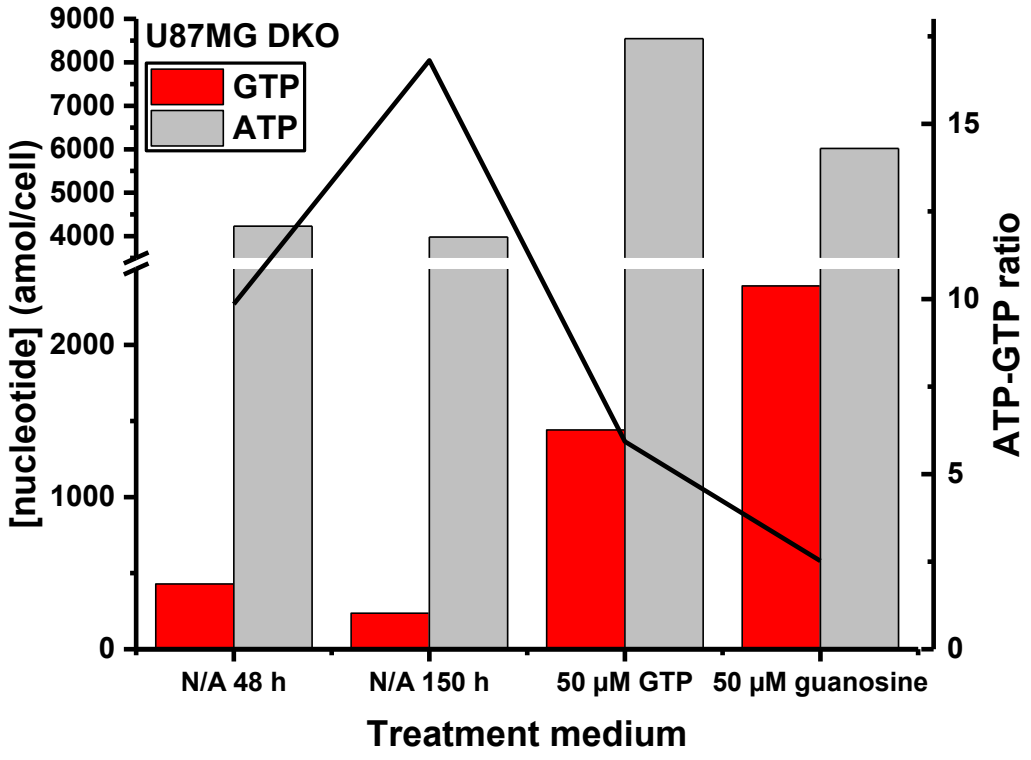

Figure 32. The results of the cell-based U87MG DKO samples.

The co-cultures were used to study the possible rescuing effect between the DKO and the WT cells. U87MG DKO cells which were co-cultured with WT cells (Figure 33) were expected to have higher GTP concentrations and lower ATP-GTP ratio when compared to DKO cells (cultured for 48 h), but the measured GTP concentrations were lower when compared to DKO cells. There was not any significant difference between the two different pore sizes (1.0 or 3.0 µm) or co-culture time. Based on these results, the possible rescuing effect can not be confirmed and optimization of the sample preparation would be needed to achieve consistent results.

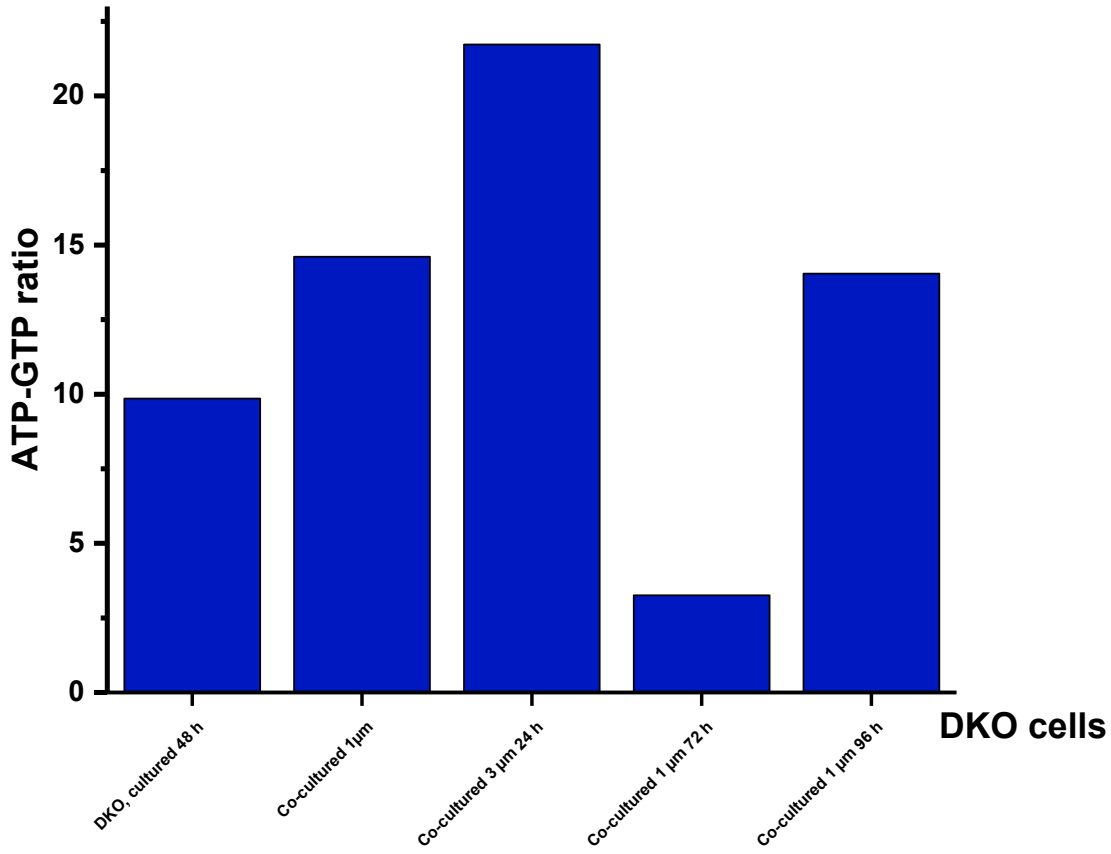

Figure 33. The results of the co-cultured DKO cells.

The presence of GTP and ATP in the culture medium was studied shortly. 10 mL of the culture medium was collected from WT culture, DKO culture and co-culture. The medium was dried and dissolved again in MQ. The results of the GTP measurement were normalized and compared to the GTP signal which was measured from the medium sample from the bottle (Figure 34). This control sample was dried and dissolved similarly to other samples. Most of the signals of the medium samples were not in the linear range of the assay and the dilution factor was too low. Based on these results, there was GTP in the culture medium. The highest concentration was measured from the WT culture and the lowest from the medium from the DKO culture. The GTP level of the medium from co-culture was in between the WT and DKO. It is also possible that other components in the medium were also disrupting the GTP detection. The measured background was high in this assay, even the medium sample from the medium bottle had a signal level respective to 750 nM of GTP, and the rest of the samples had more. This high background would indicate there were disrupting compounds in the control medium and also the used dilution factor for the samples was too low. Nevertheless, described differences were detected between the culture medium samples. The measured ATP level (not shown) was close to 0 (below the 4 nM standard point). Based on this, there was no ATP or similar disrupting compounds in the medium of the cultures.

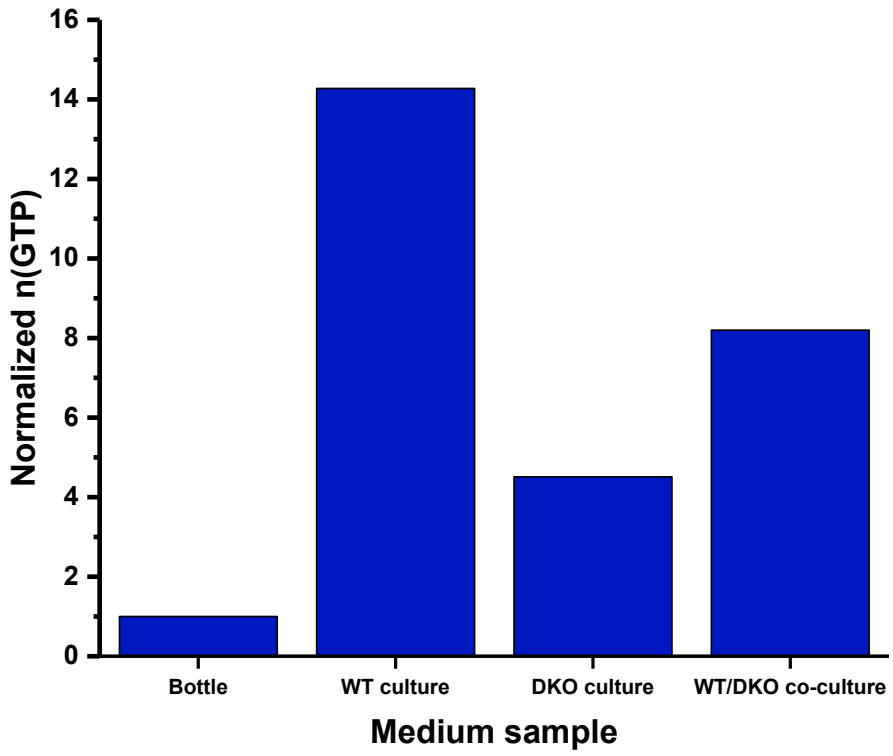

Figure 34. Results of the GTP measurements from the medium samples. The results are normalized to the level of signals measured from the medium bottle.

The direct GTP-ATP assay was used to measure the concentrations of the free GTP and ATP from the diluted cell lysate. In this homogenous assay, the GTP of the sample and the produced Eu^{3+}-chelate labelled GTP competes in binding to anti-GTP Fab2A4 and a soluble quencher molecule MT2 is quenching the TRL-signal of the free Eu^{3+}-chelate-GTP (ex. 340 nm, em. 620 nm) in the solution. When combined with a commercial ATP kit, the ATP-GTP ratios were studied, giving more information about the energetic state of the cells. The concentrations from the WT cells and GTP biosynthesis deficient DKO cells were monitored after different treatments and after co-culture. Differences in ATP-GTP ratio in WT cells after different treatments were detected. When compared to the control sample (0.1% DMSO) with a ratio of 7–8, 50 µM guanosine treatment decreased the ratio by increasing the GTP concentration. 10 µM MPA treatment increased the ratio because of the decreasing GTP concentration. The timeline of the MPA treatment was also measured in 8 time points. The effect of MPA treatment was achieved after 4–6 h and it stayed constant only slightly decreasing throughout the monitoring period until 120 h. In DKO cells the ATP-GTP ratio of untreated samples was higher (10–17) than in WT cells due to the lower GTP concentration. After the addition of 50 µM GTP, the ratio decreased to 5 and with 50 µM guanosine, the ATP-GTP ratio decreased to 2.5 and the GTP concentration increased more when compared to GTP-treated cells. The co-culture of WT and DKO cells was an important step although the possible rescuing effect was not confirmed and optimization of the sample preparation would be needed to achieve consistent results. The presence of GTP was also detected in the medium samples. Medium samples from different cultures would be needed to study more closely to establish if there are GTP or other assays disrupting compounds explaining the different signal levels in WT, DKO and co-culture mediums.

The achieved results were on line when compared to the literature, where the ATP-GTP ratio is approximately 10.9 in the cells of the cell culture, 7.5 in tissue and 6.6 in tumor cells.[12] In this case, the cultured U87MG WT cells are glioblastoma tumor cells and their measured ATP-GTP ratio was 7–8, which is close to the values found in the literature. The cultured U87MG DKO cells are closer to normal cells than WT cells since their ability to produce GTP is reduced and they are not proliferating as rapidly. Based on the literature, their ATP-GTP ratio should be higher than in tumor cells, and this was proved since the measured ATP-GTP ratio of DKO cells was 10 (cultured 48 h) and 17 (cultured 150 h).

4 Conclusions

Two methods were developed to detect GTP with the GTP-specific Fab fragment in glioblastoma cells. In bioimaging, the anti-GTP Fab fragment was successfully used to image directly GTP from the fixed cells. The Fab2A4m variant showed improved functionality in comparison to Fab2A4 because it is a matured variant and therefore has a higher affinity to GTP. The developed staining method was used in multicolour immunostaining to image IMPDH2 with commercial antibodies simultaneously. Various secondary antibodies were tested and optimisation was needed to find the suitable secondary antibody. The Fab was able to be used with IgG AF488 as a secondary antibody in low dilution (1:1000) but had clear fluorescence signals and showed clear differences which were in line with the IMPDH2 results. Differences were detected in GTP and IMPDH2 signals after different treatments and between U87MG WT and DKO cells.

Fab2A4 was utilized in a high throughput 384-format to quantify the GTP concentration in a linear range of 10-1 000 nM obtained from the cell-based samples. In the GTP-ATP assay, the GTP of the sample and the Eu^{3+}-chelate-GTP compete in binding to the anti-GTP Fab fragment. With the addition of the commercial ATP kit, the energy metabolic state of the cells can be described with high sensitivity. With the GTP-ATP assay, the ATP-GTP ratios of U87MG WT and DKO cells were monitored after treatments. The sample preparation for the assay has advantages when compared to traditional separation-based methods, such as HPLC-MS. The cell lysate can be used in the assay without the need for time-consuming separation steps, only short centrifugation is needed. Therefore GTP-ATP assay has a high capability to study a wide range of biological samples and molecular interactions. It is a rapid tool for biochemical studies and has also high sensitivity due to the used Eu^{3+}-chelate.

The achieved results of IMPDH2 and GTP imaging and measured ATP-GTP ratios were compared after different treatments and between U87MG WT and IMPDH1/2-DKO cell strains. From the MPA-treated cells, the detected fluorescence signal from GTP was diminished and the IMPDH2 staining showed the RR effect. The measured ATP-GTP ratio was significantly increased from the level of the control sample 7-8 to 13 due to the decreased GTP and slightly increased ATP as well. The affect of MPA can first be noticed in IMPDH-enzymes and it is delayed in the concentration of GTP. From the guanosine-treated cells, the detected fluorescence from GTP and IMPDH2 was brighter when compared to the control samples. The guanosine treatment was tested in two concentrations, 50 µM and 100 µM. The

preliminary tests with crystal violet assay and also the GTP-ATP assay tests showed disadvantageous results with the 100 µM guanosine concentration which could indicate the possible toxic effect caused by too high guanosine concentration. Therefore 50 µM guanosine was selected for use in further tests with the GTP-ATP assay. The GTP level increased in guanosine-treated WT cells, but it did not decrease the ATP-GTP ratio significantly. On the other hand, with DKO cells the guanosine treatment decreased the ATP-GTP ratio from 10-15 to 2. In DKO cells, the guanosine treatment seems not only to return the cells close to the control level of the WT samples (ratio 7-8) but also improve their GTP production over this level. In comparison to WT cells, the detected low signals from DKO cells required multiple times longer exposure times. Even with the longer exposure time, the fluorescence signal was very diminished when compared to clear signals from WT cells with shorter times. This indicates that the levels of GTP and IMPDH2 are very low when compared to WT cells. With the GTP-ATP assay, the measured nucleotide ratio differs significantly between these two strains. In the WT cells the ATP-GTP ratio was 7-8 and in DKO cells 10-15. The ratio of the MPA-treated cells (12-15) can be comparable with the ratio of the DKO cells. This would indicate that MPA treatment can mimic the functional state of the DKO cells.

In the future, the structural analysis of the Fab fragment would be highly needed. The quaternary structure of the Fab fragment could give valuable information about its binding regions to the binding groups of GTP. This could be combined with the structural information of the catalytic binding site of intracellular GTP-sensor PI5P4Kβ, to resolve the GTP-specific binding forces (kinase also binds to ATP).[5] This could represent a desirable structure and lead to the development of more effective GTP binders.

For imaging purposes, the conjugation of the Fab2A4m with the fluorescent dye would be a beneficial future aspect. Separate fluorescent secondary antibodies are usually used, because of the convenient compatibility with various primary antibodies. Because the GTP imaging results depended largely on the ability of the secondary antibody to bind the Fab fragment, it would be advantageous to conjugate the Fab with the dye and use it in direct imaging of GTP. In addition to imaging, the fluorophore labelled Fab fragment could be used in other applications as well. For example, a non-competitive format fluorescence polarization assay (FPIA) could utilize the labelled Fab fragment to detect GTP concentration in a homogenous solution.

The next step in the development of the GTP-ATP assay would be to simplify the sample preparation process to make it faster. It would be advantageous to culture the cell-based samples and be able to use the developed assay in the same well plate without increasing the consumption of the detection solution too much. The obstacles in this are the cell lysis required for the homogenous assay and the residues of the organelles in the lysate which would be needed to centrifuge down and could disrupt the detection of GTP. Also, an important step would be to screen a wider range of different cell lines with GTP-ATP assay to confirm its capacity and to gain information on the GTP-ATP concentrations and ratio in various cell lines. Would be also valuable to screen the GTP-ATP ratios in different conditions, for example WT and DKO cells under starvation (no glucose) to study their regulation of energy molecules in different environments since the concentrations of nucleotides vary not only by tissue type but also by environment.[5]

Different kinds of information can be reached with qualitative analysis of bioimaging and quantitative analysis of GTP-ATP assay. By combining the information from two different sources it is possible to get more information about the cellular phenomena, the cell's energetic state and its regulation. For example, imaging informs about the localization and the GTP-ATP assay about the exact nucleotide concentrations and their intracellular ratio. These applications can be used as complementary tools or separately, depending on the purpose. In the future, both methods would benefit the investigation of new drug targets in cancer research and the development of cancer drugs.

References

1. Brown, P. R. *HPLC in nucleic acid research: methods and applications*. 1st edition; Chromatographic science series vol. 28; Marcel Dekker; New York, USA, 1984, p. 7–53, 239–240.
2. Alberts, B.; Bray, D.; Hopkin, K.; Johnson, A.; Lewis, J.; Raff, M.; Roberts, K.; Walter, P. *Essential Cell Biology*. 4. painos; New York, NY: Garland Science, 2014, p. 59, 77, 421, 541.
3. Haug, E.; Sjaastad, Ø. V.; Sand, O.; Toverud, K. C. *Ihmisen fysiologia.* 5th edition*;* SanomaPro, 2012, p. 4–101.
4. Kopra, K.; Härmä, H. *N. Biotechnol.* **2015**, *32*, 575–580.
5. Sumita, K.; Lo, Y.; Takeuchi, K.; Senda, M.; Kofuji, S.; Ikeda, Y.; Terakawa, J.; Sasaki, M.; Yoshino, H.; Majd, N.; Zheng, Y.; Kahoud, E. R.; Yokota, T.; Emerling, B. M.; Asara, J. M.; Ishida, T.; Locasale, J. W.; Daikoku, T.; Anastasiou, D.; Senda, T.; Sasaki, A. T. *Mol. Cell* **2016**, *61*, 187–198.
6. Kofuji, S.; Sasaki, A. T. *J. Biochem.* **2020**, *168*, 319–328.
7. Schiavon, C. R.; Griffin, M. E.; Pirozzi, M.; Parashuraman, R.; Zhou, W.; Jinnah, H. A.; Reines, D. Kahn, R. A. *Mol. Biol. Cell* **2018**, *29*, 2303–2316.
8. Allen, M.; Bjerke, M.; Edlund, H.; Nelander, S.; Westermark, B. *Sci. Transl. Med.* **2016**, *8*, 354.
9. Kofuji, S.; Hirayama, A.; Eberhardt, A. O.; Kawaguchi, R.; Sugiura, Y.; Sampetrean, O.; Ikeda, Y. Warren, M.; Sakamoto, N; Kitahara, S.; Yoshino, H.; Yamashita, D.; Sumita, K.; Wolfe, K.; Lange, L.; Ikeda, S.; Shimada, H.; Minami, N.; Malhotra, A.; Morioka, S.; Ban, Y.; Asano, M.; Flanary, V. L.; Ramkissoon, A.; Chow, L. M. L.; Kiyokawa, J.; Mashimo, T.; Lucey, G.; Mareninov, S.; Ozawa, T.; Onishi, N.; Okumura, K.; Terakawa, J.; Daikoku, T.; Wise-Draper, T.; Majd, N.; Kofuji, K.; Sasaki, M; Mori, M.; Kanemura, Y, Smith, E. P.; Anastasiou, D.; Wakimoto, H.; Holland, E. C.; Yong, W. H.; Horinski, C.; Nakano, I.; DeBerardinis, R. J.; Bachoo, R. M.; Mischel, P. S.; Yasui, W:; Suematsu, M.; Saya, H.; Soga, T.; Grummt, I.; Bierhoff, H.; Sasaki, A. T. *Nat. Cell Biol.* **2019**, *21*, 1003–1014.
10. Calise, S. J.; Purich, D. L.; Nguyen, T.; Saleem, D. A.; Krueger, C.; Yin, J. D.; Chan, E. K. L. *J. Cell Sci.* **2016**, *129*, 3042–3052.
11. Ji, Y. S.; Gu, J. J.; Makhov, A. M.; Griffith, J. D.; Mitchell, B. S. *J. Biol. Chem.* **2006**, *281*, 206–212.

12. Traut, T. W. *Mol. Cell. Biochem.* **1994**, *140*, 1–22.
13. Lush, C.; Rahim, Z. H. A.; Perrett, D.; Griffiths, J. R. *Anal. Biochem.* **1979**, *93*, 227–232.
14. Reinhart, M. P.; Koroly, M. J. *Anal. Biochem.* **1982**, *119*, 392–396.
15. Hall, M. D.; Yasgar, A.; Peryea, T.; Braisted, J. C.; Jadhav, A.; Simeonov, A.; Coussens, N. P. **2017**, *4*, 1–41.
16. Morrison, L. E. *Anal. Biochem.* **1988**, *174*, 101–120.
17. Wang, Q.; Nono, K. N.; Syrjänpää, M.; Charbonniere, L. J.; Hovinen, J.; Härmä, H. *Inorg. Chem.* **2013**, *52*, 8461–8466.
18. Smith, D. S.; Eremin, S. A. *Anal. Bioanal. Chem.* **2008**, *391*, 1499–1507.
19. Lea, W. A.; Simeonov, A. *Expert Opin. Drug Discov.* **2011**, *6*, 17–32.
20. Bianchi-Smiraglia, A., Rana, M. S., Foley, C. E., Paul, L. M., Lipchick, B. C., Moparthy, S., Moparthy, K., Fink, E. E., Bagati, A., Hurley, E., Affronti, H. C., Bakin, A. V., Kandel, E. S., Smiraglia, D. J., Feltri, M. L., Sousa, R.&Nikiforov, M. A., *Nat. Methods* **2017**, *14*, 1003–1009.
21. Kopra, K.; Rozwandowicz-Jansen, A.; Syrjänpää, M.; Blazevits, O.; Ligabue, A.; Veltel, S.; Lamminmäki, U.; Abankwa, D. Härmä, H. *Anal. Chem.* **2015**, *87*, 3527–3534.
22. Kopra, K.; Adrichem, A. J. van; Salo-Ahen, O. M. H.; Peltonen, J.; Wennerberg, K.; Härmä, H. *Anal. Chem.* **2017**, *89*, 4508–4516.
23. BellBrooksLabs: Transcreener® GDP FP Assay https://www.bellbrooklabs.com/products/transcreener-hts-assays/gdp-gtpase-assays/gdp-assay-fp/. (25.05.2023).
24. ThermoFisher: The AlexaFluor dyes https://www.thermofisher.com/us/en/home/references/molecular-probes-the-handbook/technical-notes-and-product-highlights/the-alexa-fluor-dye-series.html. (25.05.2023).
25. BellBrooksLabs: Transcreener® GDP-GTP ase assays https://www.bellbrooklabs.com/products/transcreener-hts-assays/gdp-gtpase-assays/. (25.05.2023).
26. Sigma-Aldrich: Malachite Green Phosphate Assay Kit https://www.sigmaaldrich.com/catalog/product/sigma/mak307?lang=fi&region=FI. (25.05.2023).

27. PubChem: Malachite green https://pubchem.ncbi.nlm.nih.gov/compound/malachite_green#section=Related-Compounds. (04.06.2023).
28. Shutes, A.; Der, C. J. *Methods* **2005**, *37*, 183–189.
29. Promega: CellTiter-Glo® Luminescent Cell Viability Assay Technical Bulletin https://fi.promega.com/resources/protocols/technical-bulletins/0/celltiter-glo-luminescent-cell-viability-assay-protocol/. (04.06.2023).
30. Promega: CellTiter-Glo® https://fi.promega.com/products/cell-signaling/gpcr-signaling/gtpase-glo-assay/?catNum=V7681. (04.06.2023).
31. AAT Bioquest: ATP kit https://www.aatbio.com/products/readiuse-rapid-luminometric-atp-assay-kit?gclid=EAIaIQobChMIvPrSztbb6wIVFc53Ch2lqgJpEAAYASAAEgLVlPD_BwE. (04.06.2023).
32. Chen, P.; Liu, Z.; Liu, S.; Xie, Z.; Aimiuwu, J.; Pang, J.; Klisovic, R.; Blum, W.; Grever, M. R.; Marcucci, G.; Chan, K. K. *Pharm. Res.* **2009**, *26*, 1504–1515.
33. Riekkola, M.-L.; Hyötyläinen, T. *Kolonnikromatografia ja kapillaarielektromigraatiotekniikat.* 2. edition; Helsingin yliopisto, Analyyttisen kemian laboratorio, 2002, p. 4–33, 97, 137–183, 327.
34. Kampen, J. J. A. van, Fraaij, P. L. A.; Hira, V.; van Rossum, A. M. C.; Hartwig, N. G.; de Groot, R.; Luider, T. M. *Biochem. Biophys. Res. Commun.* **2004**, *315*, 151–159.
35. Hillebrand, S.; Garcia, W.; Cantu, M. D.; de Araujo, A. P. U.; Tanaka, M.; Tanaka, T.; Garratt, R. C.; Carrilho, E. *Anal Bioanal Chem.* **2005**, *383*, 92–97.